

Review

Open Access



# Recent advances in porous adsorbent assisted atmospheric water harvesting: a review of adsorbent materials

Shuai Zhang<sup>1,2</sup>, Jingru Fu<sup>1,2</sup>, Guolong Xing<sup>1,2</sup>, Weidong Zhu<sup>1,2</sup>, Teng Ben<sup>1,2,\*</sup>

<sup>1</sup>Zhejiang Engineering Laboratory for Green Syntheses and Applications of Fluorine-Containing Specialty Chemicals, Institute of Advanced Fluorine-Containing Materials, Zhejiang Normal University, Jinhua 321004, Zhejiang, China.

<sup>2</sup>Key Laboratory of the Ministry of Education for Advanced Catalysis Materials, Institute of Physical Chemistry, Zhejiang Normal University, Jinhua 321004, Zhejiang, China.

\*Correspondence to: Prof. Teng Ben, Zhejiang Engineering Laboratory for Green Syntheses and Applications of Fluorine-Containing Specialty Chemicals, Institute of Advanced Fluorine-Containing Materials, Zhejiang Normal University, Yingbin avenue 688, Jinhua 321004, Zhejiang, China; Key Laboratory of the Ministry of Education for Advanced Catalysis Materials, Institute of Physical Chemistry, Zhejiang Normal University, Yingbin avenue 688, Jinhua 321004, Zhejiang, China. E-mail: tengben@zjnu.edu.cn

**How to cite this article:** Zhang S, Fu J, Xing G, Zhu W, Ben T. Recent advances in porous adsorbent assisted atmospheric water harvesting: a review of adsorbent materials. *Chem Synth* 2023;3:10. <https://dx.doi.org/10.20517/cs.2022.40>

**Received:** 8 Dec 2022 **First Decision:** 10 Jan 2023 **Revised:** 30 Jan 2023 **Accepted:** 16 Feb 2023 **Published:** 23 Feb 2023

**Academic Editor:** Wei Li **Copy Editor:** Ke-Cui Yang **Production Editor:** Ke-Cui Yang

## Abstract

Water shortage is an increasing threat to humankind. Porous sorbent assisted atmospheric water harvesting (psaAWH) has emerged as an effective technological countermeasure. In this review, we summarize the types of porous adsorbents used in psaAWH and provide an overview of their states of development. The water adsorption mechanism and the processes associated with each material are analyzed, and the application prospects of the adsorbents are evaluated. The effect of the inherent properties (pore size, functional group, etc.) of the adsorbent on the water harvesting performance is also discussed. Further, we focus on the water adsorption/desorption kinetics of the adsorbents and outline various methods to improve the kinetics. At this stage, there are many strategies for improving the kinetics of the adsorbent, which in turn influences the adsorption process and intra/inter-crystalline diffusion. However, there is still limited research on the transport of water molecules in microporous adsorbents for psaAWH. Thus, this aspect is re-examined herein from a new perspective (superfluidity) in the review. Based on the discussion, we can reasonably infer that water molecule superfluidity can exist in nanoconfined channels, thus promoting the rapid transport of water molecules. The formation of water superfluidity is a feasible strategy for improving the intracrystalline diffusion of the psaAWH adsorbent. Finally, we consider the future developments and challenges of psaAWH in detail. We think this review can serve as a guide



© The Author(s) 2023. **Open Access** This article is licensed under a Creative Commons Attribution 4.0 International License (<https://creativecommons.org/licenses/by/4.0/>), which permits unrestricted use, sharing, adaptation, distribution and reproduction in any medium or format, for any purpose, even commercially, as long as you give appropriate credit to the original author(s) and the source, provide a link to the Creative Commons license, and indicate if changes were made.



for further research in this ever-expanding field.

**Keywords:** Atmospheric water harvesting, porous adsorbent, kinetic process, superfluidity

## INTRODUCTION

Since the beginning of the 21st century, water scarcity has become a serious global resource problem<sup>[1]</sup>. Humanity persists for millennia without petrochemicals but cannot without water; however, by 2025, 1.9 billion people in the world will experience a severe freshwater crisis<sup>[2]</sup>. The world's abundant water resources maintain a poised ecological balance and considerable biodiversity, but only 2.5 percent of them are freshwater<sup>[3]</sup>. Furthermore, the most abundant freshwater reserves exist as inaccessible glaciers distributed in the northern and southern poles<sup>[4,5]</sup>. The irreconcilable conflicts between limited water resources and accelerating global economic and population growth foreshadow famines, the spread of diseases, and wars; the continued existence of humanity may depend on increased freshwater production.

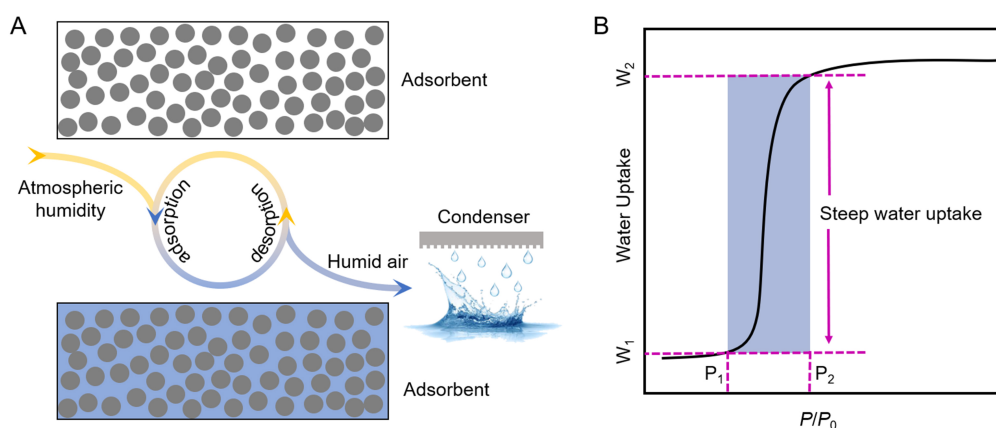
Currently, various technologies exist that can be used to produce fresh water to alleviate water crises, such as wastewater treatment, seawater desalination, and rainwater collection. Geographic or weather dependencies restrict freshwater production technologies such as seawater desalination and rainwater collection<sup>[2,6]</sup>. Wastewater treatment technology based on adsorption or membrane separation is used to purify polluted liquid water<sup>[7-11]</sup>. Although it is not restricted by geography and climate, it requires a large amount of liquid water in the local area, which indirectly restricts its application in areas of water shortage. Therefore, existing technology cannot fundamentally solve the problem of water shortage in remote water shortage areas. Atmospheric humidity, one of the three major water sources in the world, is abundant, ubiquitous, and can be replenished in a timely manner through global atmospheric circulation<sup>[1]</sup>. If freshwater can be produced directly from atmospheric humidity, it will fundamentally solve the global water shortage problem. Thus, atmospheric water harvesting (AWH) technology, which harvests freshwater from air humidity, is considered an effective solution to the water shortage problem<sup>[12-15]</sup>. The three major AWH techniques include condensation (*i.e.*, cooling air below its dew point), fog collection, and porous sorbent assisted AWH (psaAWH)<sup>[13,16]</sup>.

Fog collection must be performed in areas where fog often occurs, which is not suitable for arid areas<sup>[2]</sup>. For condensation, at the beginning of condensation, the associated sensible heat must be removed to condense the air to the dew point, and then some latent heat is required to complete the transition of water from a gaseous state to a liquid state. To collect a certain amount of water, the value of latent heat is usually certain and inevitable, which is related to the characteristics of the material itself. By contrast, the sensible heat required varies with the environment. Consequently, condensing water vapor into a liquid state at high temperatures and in dry conditions is very energy-intensive and even impossible to achieve in several cases<sup>[17,18]</sup>. In contrast, psaAWH has climatic flexibility for widespread applications owing to the diverse water adsorption characteristics of different porous materials, which is considered to be the development trend of AWH technology<sup>[19-21]</sup>. The characteristics of several freshwater production technologies are summarized in [Table 1](#).

The process and mechanism of action of psaAWH are shown in [Figure 1A](#). In general, psaAWH produces freshwater in three steps<sup>[16]</sup>. First, water in the gas phase of the atmosphere is adsorbed by porous materials and stored in the channel in the form of a bulk phase to realize the enrichment of atmospheric water. Second, water is released over time through external stimuli, such as light or heat, to a confined space. With the continuous release of water from the porous adsorbent, this space increases in humidity relative to the

**Table 1. Summary of characteristics of several freshwater production technologies**

Technology name	Geographic dependencies	Weather dependencies	Implementation premise
Seawater desalination	Yes	No	Coastal
Rainwater collection	No	Yes	Rainfall
Fog collection	No	Yes	Foggy
Condensation	No	Yes	Difficult to implement at low RH
psaAWH	No	No	Presence of atmospheric humidity

**Figure 1.** (A) Water production process of psaAWH; (B) water release mechanism of porous materials in psaAWH.

external atmosphere, which significantly reduces the sensible heat required for the condensation process. Finally, the moist air can be easily cooled and condensed into liquid water. Therefore, if psaAWH is to be implemented in a certain climate, the porous adsorbent must possess the ability to adsorb atmospheric water at the relative humidity (RH) of the climate, which can be verified using the water vapor adsorption isotherm. As shown in Figure 1B, the abscissa is the relative partial pressure of water vapor (RH), and the ordinate is the water vapor adsorption capacity of the porous materials. Under ambient RH ( $P_2$ ), the porous material exhibited higher water uptake ( $W_2$ ). With external stimulation (such as increasing temperature), the RH around the porous material decreased to  $P_1$ . At this time, the water uptake decreased to  $W_1$ , and excess water molecules were released into a closed space to obtain liquid water through condensation. Therefore, the difference between  $W_2$  and  $W_1$  determines the working ability of a material.  $P_2$  is the applied RH of the adsorbent; that is, the RH of the atmosphere must be greater than  $P_2$ . Owing to the steep water uptake of the S-type (type-IV, V) vapor adsorption isotherm, it can have a high working capacity under small external RH changes [Figure 2]. In contrast, other types of water vapor adsorption isotherms often require greater RH changes to produce a better working capacity because of the lack of steep water uptake at an appropriate RH, which often implies that higher energy must be provided to heat the adsorbent<sup>[15]</sup>.

Hence, an ideal porous sorbent for psaAWH should feature: (1) an S-type water vapor adsorption isotherm at the required RH; (2) high water uptake to maximize water production per cycle; (3) rapid adsorption/desorption kinetics under lower energy consumption to maximize the circulation rate; and (4) structural resilience to multiple water adsorption/desorption cycles. To date, much effort has been devoted to the development of porous adsorbents with high psaAWH performances. However, the diversity of adsorbent types and modification strategies makes it difficult for us to intuitively understand their structure-activity relationships. The summary of the structure-activity relationship of adsorbents has considerable guiding significance for future research. At present, some reviews have summarized this and

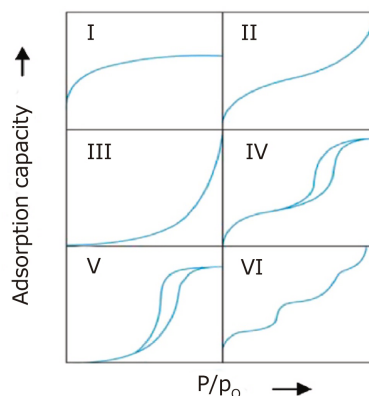


**Figure 2.** IUPAC classification of water vapor adsorption isotherms. Reproduced with permission<sup>[24]</sup>. Copyright Elsevier.

put forward prospects<sup>[13,16,22]</sup>. However, how to improve the transport speed of water molecules in the adsorbent micropores should be discussed, which is expected to promote the further development of psaAWH. In addition, other reviews have less attention to the emerging materials such as covalent organic frameworks (COFs) and crystalline porous organic salts (CPOs)<sup>[5,22-24]</sup>.

Therefore, in this review, we begin with a summary of the materials used in psaAWH and analyze the advantages and disadvantages of each material. Then, we discuss the effects of the inherent properties of porous adsorbents, such as pore size and functionality, *etc.*) on psaAWH performance and provide a general design idea for the preparation of the required adsorbent. In the adsorption/desorption kinetics of porous adsorbents, we discuss various design strategies to improve the kinetic process. In particular, we focus on the kinetics of water molecules in the microporous channel. Finally, we discuss the future development of psaAWH adsorbents and offer suggestions to solve their current problems. Through an analysis of the mechanism of water superfluidity, reasonable suggestions are proposed on how to improve the kinetics of microporous adsorbents.

## CATEGORIES OF POROUS ADSORBENTS

The psaAWH can be tuned to specific climatic conditions by tuning the structure of its porous materials. Therefore, various porous materials can be used for psaAWH. An overview of the categories of porous materials used in psaAWH<sup>[25-30]</sup> is presented in this section. The development history of the main porous materials used in psaAWH is shown in Figure 3<sup>[27,29,31-37]</sup>, which includes the following categories.

### Classic materials

For most classic adsorbent materials (such as silica gel and zeolites), the adsorption of water vapor is due to their hydrophilicity. When in contact with water molecules, the adsorption site on the inner surface of the adsorbent channel attracts and adsorbs water molecules entering the channel and fixes them on the inner surface of the channel [Figure 4]. If there is still space for water molecules in the adsorbent, the subsequent water molecules will be adsorbed by unsaturated adsorption sites or existing water molecules in the channel, leading to pore filling. In the desorption process, the desorption sequence of water molecules is generally the reverse of that of adsorption.

Silica gel, an amorphous porous material composed of  $\text{SiO}_2$  and  $\text{H}_2\text{O}$ , exhibits selective water adsorption<sup>[23]</sup>. It has been widely studied as a common water-adsorbing material<sup>[38]</sup>. In silica gel, the hydroxyl groups in silanol groups (Si-OH) are the main sites for the adsorption of water molecules. Water molecules are fixed

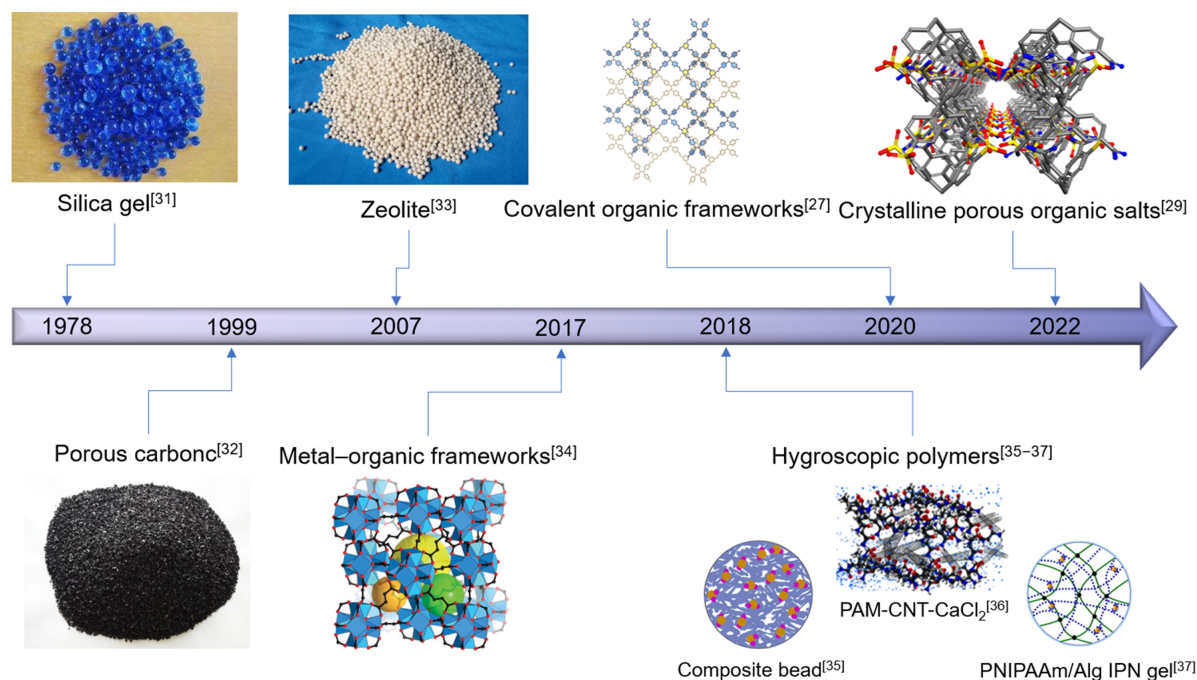


**Figure 3.** Development history of psaAWH. Silica gel<sup>[31]</sup>. Porous carbon<sup>[32]</sup>. Zeolite<sup>[33]</sup>. Metal-organic frameworks. Reproduced with permission<sup>[34]</sup>. Copyright The American Association for the Advancement of Science. Composite bead. Reproduced with permission<sup>[35]</sup>. Copyright Springer Nature. PAM-CNT-CaCl<sub>2</sub>. Reproduced with permission<sup>[36]</sup>. Copyright American Chemical Society. PNIPAAm/Alg IPN gel. Reproduced with permission<sup>[37]</sup>. Copyright Springer Nature. Covalent organic frameworks. Reproduced with permission<sup>[27]</sup>. Copyright American Chemical Society. Crystalline porous organic salts. Reproduced with permission<sup>[29]</sup>. Copyright John Wiley and Sons.

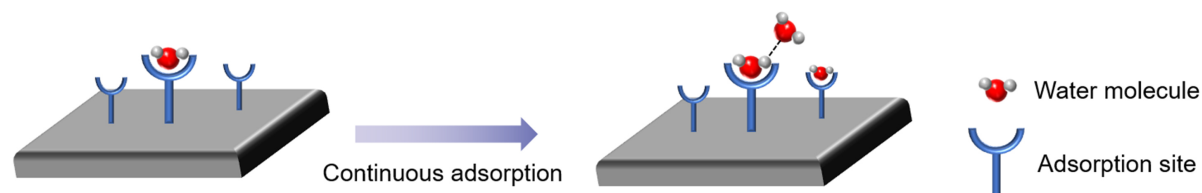


**Figure 4.** Water adsorption process of mainly classic materials.

on the surface of the silica gel channel by forming hydrogen bonds with the hydroxyl groups. However, the water uptake of silica gel is generally low, particularly at low RH, which limits its application in psaAWH<sup>[39,40]</sup>.

Zeolites are crystalline porous materials that are typically composed of aluminum oxide, silicon dioxide, and counterions. They feature crystal channels with high polarity and electrostatic charge that facilitate good water adsorption<sup>[41-44]</sup>. Because of the existence of framework anions and counterions in molecular sieves, they usually possess multiple water adsorption sites, including Lewis acid sites (framework anions), Brønsted acid sites (bridging hydroxyls), counterions, and defect sites<sup>[41]</sup>. Although these sites endow molecular sieves with good hydrophilicity, their attraction to water molecules is too strong, leading to zeolites usually displaying type I water vapor adsorption isotherms, which are unfavorable for psaAWH because they represent energy-intensive regeneration processes<sup>[23,45,46]</sup>. For example, Wynnyk *et al.* measured the water adsorption isotherms of zeolite 13X at temperatures ranging from 25 °C to 150 °C<sup>[45]</sup> and found them to be type I. This implies that even if the regeneration temperature is as high as 150 °C, several water

molecules cannot be completely released from the molecular sieve. To address this drawback and regulate the water adsorption process, Krajnc *et al.* synthesized a microporous LTA-type zeolite (AlPO<sub>4</sub>-LTA) that shows an S-type water vapor adsorption isotherm, owing to its accessible pore volume, indicates the potential applicability of psaAWH [Figure 5]<sup>[47]</sup>. Although the regeneration temperature of zeolites has been reduced by modification, it is still high compared to the current advanced porous materials.

Clays and organosilicas are two classic porous materials with water adsorption capacity. Clays have a layered structure composed of silica tetrahedron and alumina octahedron as the basic constituent units, and the interlayer is connected by counter-cations with a positive charge through non-covalent bond interactions. Therefore, similar to zeolites, they exhibit good hydrophilicity. However, significant interlayer swelling is easily caused after water absorption, resulting in a loss of water adsorption capacity after regeneration<sup>[41]</sup>. Usually, this problem can be solved by interlayer crosslinking or the formation of interlayer metal oxide pillared clays<sup>[48]</sup>. By constructing oxides of different metal cations (Na<sup>+</sup>, Ca<sup>2+</sup> and Mg<sup>2+</sup>) between layers, Zhu *et al.* improved the stability and water adsorption performance of clay at low RH<sup>[49]</sup>. Although clay has good water affinity, its pores are primarily derived from interlayer stacking and therefore have a low water adsorption capacity, which is not suitable for psaAWH. Organosilicas refer to a class of materials whose main chain contains silicon atoms and organic groups are directly connected to silicon atoms. Most organosilicas are hydrophobic materials; however, modification of the polymer chains can improve their hydrophilic properties and enable them to possess water adsorption capacity<sup>[50]</sup>. Mietner *et al.* studied the effect of different functional group modifications on the water adsorption performance of organosilicas<sup>[51]</sup>. The results indicate that organosilicas with an S-type water vapor adsorption isotherm can be obtained by surface modification and structural design, and the inflection point of the water vapor adsorption isotherm can be regulated by different hydrophilic groups. Currently, organosilicas show potential application value in psaAWH; however, the preparation of organosilicas with a homogeneous micropore structure is still a challenge, which makes it unsuitable for application to psaAWH at low RH.

### Metal-organic frameworks

Metal-organic frameworks (MOFs) are a structurally diverse class of classical porous materials. They are composed of metal clusters joined by organic linkers and have relatively controllable and uniform pore sizes<sup>[52,53]</sup>. Although previously designed MOFs exhibit poor stability<sup>[23]</sup>, recent MOF designs offer water stability and synthetic flexibility<sup>[54-61]</sup>.

Various MOFs with high water stability have been studied for their water-adsorption properties<sup>[62-68]</sup>. The first strategy for building a water-stable MOF is to strengthen the coordination bonds between the metal clusters and organic linkers. Accordingly, Choi *et al.* synthesized two types of zinc(II)-pyrazolate MOFs using a Brønsted base (pyrazole) to replace traditional carboxylic acids as organic linkers<sup>[69]</sup>. Because the stronger coordination interaction between pyrazole and the metal clusters effectively prevents the degradation of coordination bonds by water molecules, the two zinc(II)-pyrazolate MOFs exhibit excellent water stability. Subsequently, zeolitic imidazole frameworks (such as ZIF-8 and ZIF-68) have also demonstrated exceptional water stability<sup>[70,71]</sup>. Another effective strategy to improve the water stability of MOFs is to increase the connectivity of secondary building units (SBUs), thereby increasing the steric hindrance of the metal contact with water molecules. For this reason, Tian *et al.* synthesized a hetero-triple-walled MOF that possesses a high-connectivity SBU and shows excellent water stability<sup>[72]</sup>. In addition, high-connectivity Zr-based MOFs exhibit outstanding water stability<sup>[19]</sup>. Finally, the use of inert cations is an effective strategy for preparing water-stable MOFs<sup>[73,74]</sup>. For example, the inert Cr<sub>3</sub>O<sub>7</sub><sup>+</sup> clusters in Cr-MIL-101 significantly slow down the degradation of metal clusters by water molecules, allowing them to maintain crystallinity for months in moist air<sup>[75]</sup>.

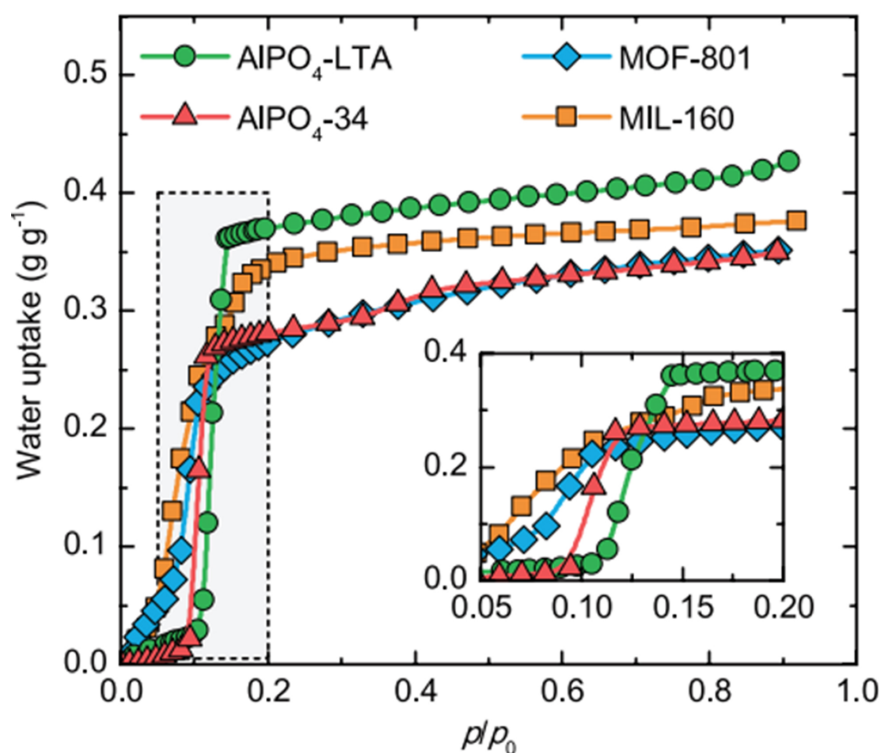


**Figure 5.** Water sorption isotherms for several adsorbents at 30 °C. Reproduced with permission<sup>[47]</sup>. Copyright John Wiley and Sons.

The adsorption of water molecules by MOFs is primarily achieved through three mechanisms. The first mechanism involves chemical adsorption of the open metal sites. After high-temperature activation to remove the coordination solvent, some MOFs expose unsaturated metal sites, which become adsorption sites for the water molecules<sup>[75]</sup>. For example, after high-temperature activation, Zr in UiO-66 exposes an unsaturated metal site, which preferentially absorbs water molecules into the pores<sup>[76]</sup>. The open metal sites in CPO-27 (i.e., MOF-74) significantly influence its water adsorption performance. Dietzel *et al.* directly observed the adsorption sites of water molecules by refining its diffraction data of CPO-27-Zn, which was controlled to desorb water molecules at different temperatures [Figure 6]<sup>[77]</sup>. The results indicate that the open metal sites can bind water molecules through strong chemical adsorption, and this portion of the water molecules can be removed only at high temperatures. In psaAWH, the sharply increased water adsorption capacity of some MOFs at low relative humidity may be owing to the strong water affinity of the open adsorption sites<sup>[78]</sup>.

Cluster adsorption is another adsorption mechanism. The prerequisite for cluster adsorption is the presence of hydrophilic sites in MOFs that serve as nucleation sites for water molecular clusters. For MOFs, the hydrophilic sites can be open metal sites or hydrophilic groups on the organic linkers. First, water molecules nucleate at the hydrophilic sites, and then the subsequent water molecules gather to form water clusters, leading to steep water uptake. Finally, the water molecules continue to fill the remaining space in the MOFs to reach adsorption saturation. Wagner *et al.* systematically studied the cluster adsorption process in ZIF-90 using theoretical calculations<sup>[68]</sup>. In the initial stage of adsorption, the nucleation of water molecules can occur only in part of the pores in ZIF-90, followed by rapid cluster growth and filling of water molecules in the pores, then the adsorption process is repeated in other pores [Figure 7A]. This result indicates that cluster growth was extremely rapid in the pores. Hanikel *et al.* also studied the cluster adsorption of water molecules in MOF-303<sup>[79]</sup>. In activated MOF-303, water molecules are adsorbed near the pyrazole and

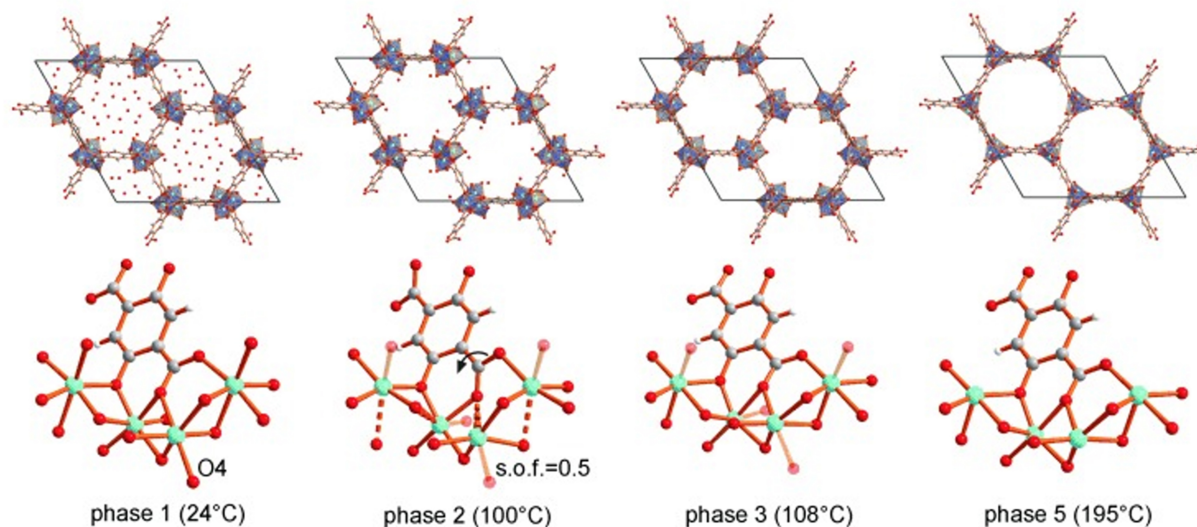


**Figure 6.** Crystal structures of the four sufficiently crystalline patterns showing the successive steps in dehydration (top) and changes in the local molecular environment (bottom). Reproduced with permission<sup>[77]</sup>. Copyright John Wiley and Sons.

hydroxyl groups through strong hydrogen-bond interactions. Subsequently, water molecules continue to grow at these nucleation sites to form water clusters and fill the pores. In fact, the adsorption mechanism of most MOFs during psaAWH is cluster adsorption, and water far away from the nucleation center is preferentially removed during desorption [Figure 7B].

Capillary condensation, which often occurs in MOFs with large pore sizes, is the final mechanism of water vapor adsorption by MOFs. According to previous reports, when the pore size of MOFs exceeds 2 nm, capillary condensation occurs easily in the pores at room temperature ( $\sim 25\text{ }^{\circ}\text{C}$ )<sup>[76]</sup>. Capillary condensation is a physical adsorption process that has weaker binding energy than chemisorption at open metal sites and can be regenerated at lower temperatures. However, note that when capillary condensation occurs, a hysteresis loop usually exists between the desorption and adsorption curves of MOFs, which is unfavorable in psaAWH because it will lead to a wider operating RH. For example, MIL-101 (Cr) has two pores with diameters of 2.9 and 3.4 nm, respectively, which results in an obvious hysteresis loop in its water vapor desorption curve [Figure 7C]<sup>[80]</sup>. Another mesoporous MOF (NU-1000) also exhibited this behavior<sup>[81]</sup>.

With the emergence of increasingly water-stable MOFs, Furukawa *et al.* first proposed utilizing MOFs as adsorbent materials for AWH in 2014<sup>[19]</sup>. In 2017, freshwater was successfully obtained from the atmosphere using MOF (MOF-801) as an adsorbent material<sup>[34]</sup>. Since this breakthrough, various MOFs have been successfully used as adsorbents for psaAWH<sup>[82-88]</sup>. Subsequently, practical psaAWH using an MOF adsorbent was performed in a desert and freshwater (0.175 kg over 24 h) was successfully harvested without providing any external energy<sup>[26]</sup>. However, although it is gratifying to successfully obtain fresh water in arid zones using MOF, such production is insufficient for sustaining human life. Incorporating hygroscopic salts (such as LiCl and CaCl<sub>2</sub>) into porous MOFs is an effective method for increasing water production<sup>[89,90]</sup>. For example, Xu *et al.* prepared a LiCl@MIL-101(Cr) composite material that displays a multi-step water sorption process, leading to excellent water production ( $0.7\text{ L kg}_{\text{adsorbent}}^{-1}\text{ d}^{-1}$ ) at relatively low humidity when combined with a light-absorbing material (carbon black; Figure 8A)<sup>[83]</sup>.

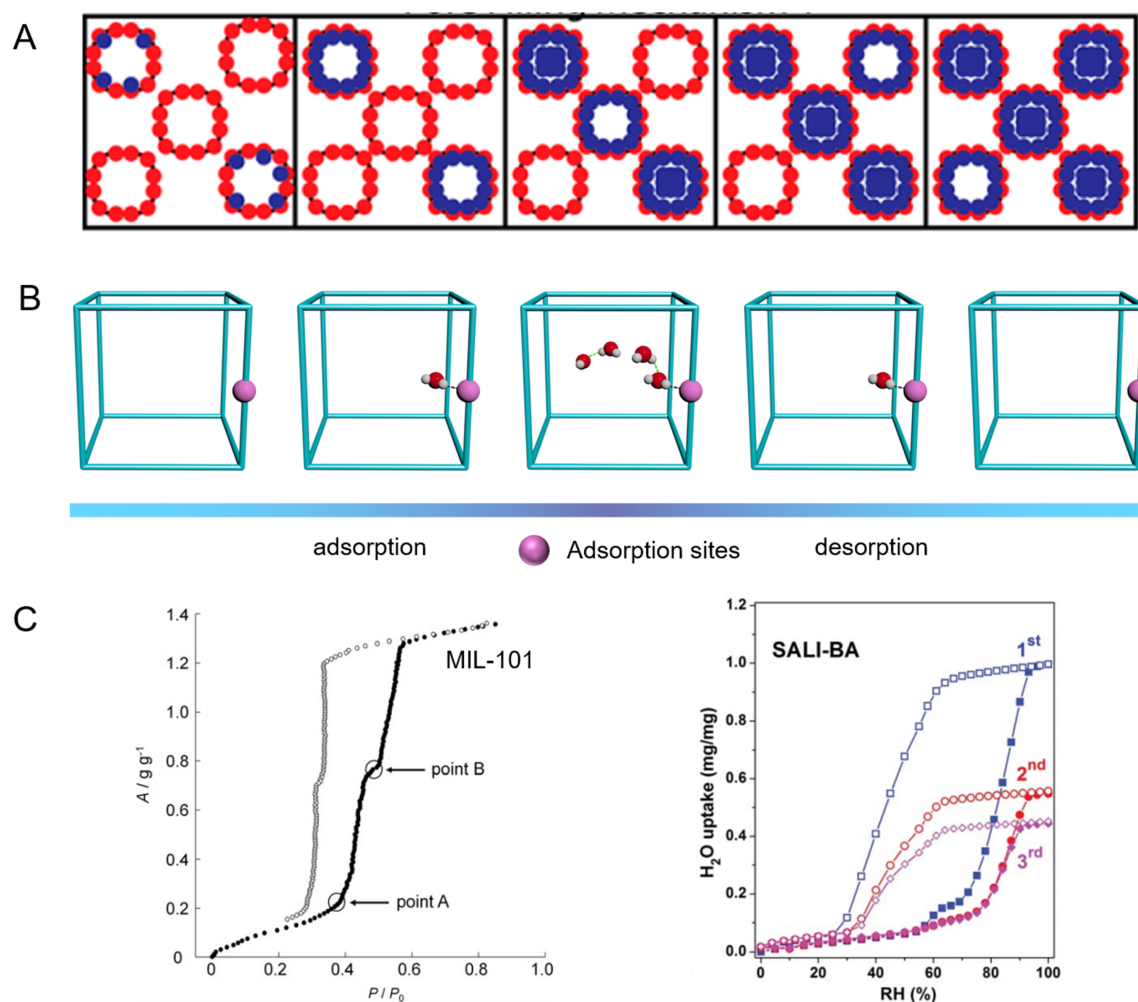


**Figure 7.** (A) Cluster mechanism, individual pores are filled before additional pores are filled. Reproduced with permission<sup>[68]</sup>. Copyright American Chemical Society; (B) the water vapor adsorption/desorption process of MOFs in psaAWH. (C) Water vapor adsorption isotherm of MIL-10<sup>[80]</sup> and SALI-modified NU-1000<sup>[81]</sup> under 25 °C. Reproduced with permission<sup>[80]</sup>. Copyright Elsevier. Reproduced with permission<sup>[81]</sup>. Copyright Royal Society of Chemistry.

To increase the cycling rate and achieve high water production, one strategy is to accelerate desorption by heating<sup>[91-93]</sup>. For example, Wu *et al.* prepared a composite cylindrical material (TUN/SA) featuring the photothermal material  $\text{Ti}_3\text{C}_2$  alongside  $\text{UiO-66-NH}_2$ . Under natural sunlight irradiation, the temperature of this material will rise rapidly, thus accelerating the release of water molecules, and a high water production can be obtained ( $57.8 \text{ mL kg}_{\text{MOF}}^{-1} \text{ h}^{-1}$ )<sup>[86]</sup>. Although the water production of MOF-based psaAWH can be increased by heating the adsorbent, most MOFs require heating above 80 °C to release the adsorbed water<sup>[34,92]</sup>, limiting energy efficiency and yield. Therefore, reducing the regeneration temperature of MOFs is an urgent issue. Karmakar *et al.* prepared an MOF/polymer composite material with a lower critical solution temperature (LCST; *c.a.* 40 °C)<sup>[88]</sup>. When the temperature was below the LCST, the polymer in the composite material exhibited hydrophilicity, then it changed to hydrophobicity when the temperature rose above the LCST [Figure 8B]; accordingly, the composite material can be regenerated under mild conditions (40 °C, 40% RH) and showed notable water production ( $1.4 \text{ L kg}_{\text{adsorbent}}^{-1} \text{ day}^{-1}$ ). Clearly, MOFs have made encouraging progress in the application of psaAWH, but its modest water production and uncertain toxicity hinder large-scale applications.

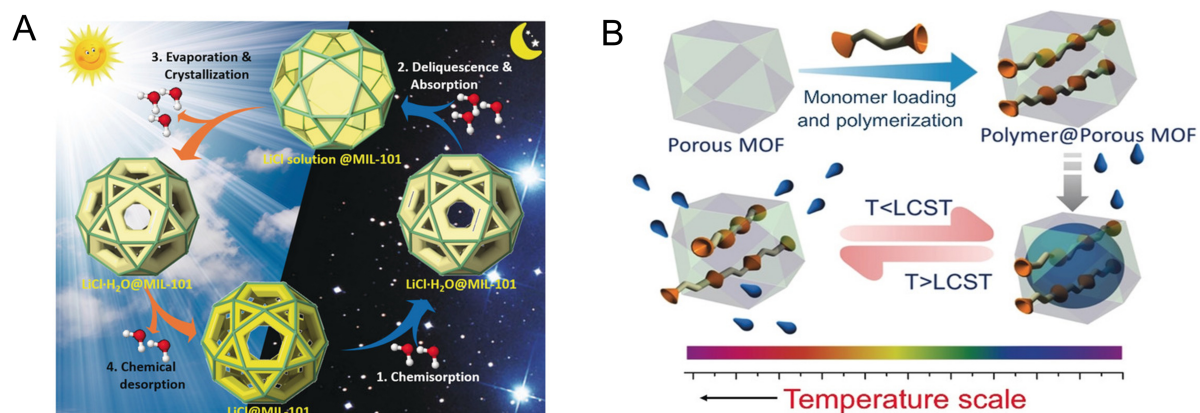


**Figure 8.** (A) Schematic of the multi-step water sorption/desorption processes of LiCl@MIL-101(Cr). Reproduced with permission<sup>[83]</sup>. Copyright John Wiley and Sons; (B) preparation of the MOF/polymer composite and the temperature-triggered water capture and release process. Reproduced with permission<sup>[88]</sup>. Copyright John Wiley and Sons.

### Covalent organic frameworks

Covalent organic frameworks (COFs) are crystalline porous materials composed of organic ligands connected by covalent bonds<sup>[94,95]</sup>. Hundreds of COFs have been widely used in a variety of fields, as reported previously<sup>[96-98]</sup>. The water adsorption performance of COFs has also been evaluated<sup>[99-107]</sup>. As a crystalline porous material, the water adsorption/desorption process of COFs in psaAWH is similar to that of MOFs [Figure 7B]. However, they do not have open metal sites, which usually cannot form strong chemisorption. Therefore, the cluster adsorption process forms the main mechanism of COFs. In COFs, the nucleation sites of water clusters generally include Schiff bases or other hydrophilic groups on the monomers. Ma *et al.* studied the adsorption of water molecules in TpPa-1 through solid-state NMR, indicating that water molecules interact with hydrophilic groups in the framework of COF pores<sup>[105]</sup>. Tan *et al.* further studied the formation of water clusters in COFs<sup>[100]</sup>. In the initial stage of adsorption, the N chain in the COFs pores serves as the nucleation site for water cluster growth, and water molecules gradually fill the entire pore from this point [Figure 9]. Similarly, when the pore size of the COF is too large, capillary condensation of water molecules will also occur, resulting in an obvious hysteresis loop between the water vapor desorption and adsorption curves<sup>[108]</sup>.

Given the recent successful applications of MOFs in psaAWH, analogous applications of COFs have drawn considerable interest, as indicated by a number of recent publications<sup>[27,109,110]</sup>. For example, in 2020, Nguyen *et al.* successfully synthesized a 2D COF (COF-432) that presented an S-type water vapor adsorption isotherm featuring a steep step in the range of 30%-40% RH [Figure 10]<sup>[27]</sup>. Owing to the square grid of mtf topology, water molecules can fill the pores of COF-432 at 40% RH, reaching a water uptake of approximately  $0.25 \text{ g}_{\text{water}} \text{ g}_{\text{adsorbent}}^{-1}$ . Moreover, COF-432 possesses ultrahigh water stability and can be regenerated at a low temperature (35 °C). At 30 °C and 40% RH, COF-432 offered an expected water production per cycle of  $0.23 \text{ g}_{\text{water}} \text{ g}_{\text{adsorbent}}^{-1}$ . However, because COFs are developing porous materials, they are underutilized in psaAWH. In addition, the high cost and harsh synthetic conditions restrict its commercial application.

### Hygroscopic polymers

Hygroscopic polymers are also common porous materials that exhibit high water adsorption capacities because of their abundant surface and bulk hydrophilic groups<sup>[111]</sup>. Hygroscopic polymers, particularly hydrogels, primarily rely on layer adsorption and capillary condensation to achieve the adsorption of water

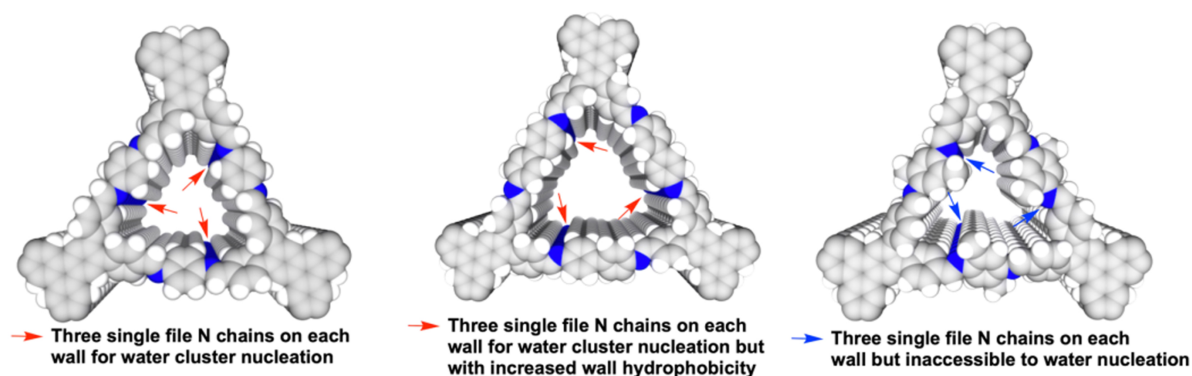


Figure 9. Nucleation site of water cluster in three COFs pore. Reproduced with permission<sup>[100]</sup>. Copyright Springer Nature.

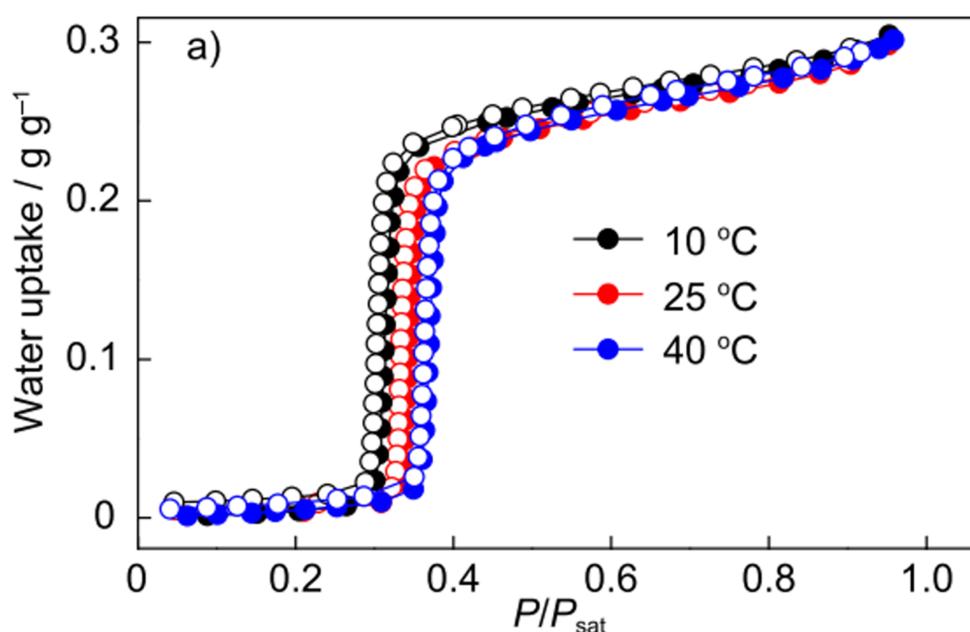


Figure 10. Water vapor adsorption isotherm of COF-432 at different temperatures. Reproduced with permission<sup>[27]</sup>. Copyright American Chemical Society.

molecules because their pores are mostly mesoporous and macroporous<sup>[112]</sup>. First, they used hydrophilic sites on the pore surface to capture water vapor and form a molecular water layer. At this instant, the adsorbed water molecules can be used as active sites to induce the subsequent multilayer adsorption of water molecules. Finally, capillary condensation occurs in various nanoscale pores to adsorb water vapor. During the nucleation stage of layer adsorption, hydrophilic groups (such as hydroxyl and carboxylic acid) in the pores of hygroscopic polymers can be used as nucleation sites<sup>[113]</sup>. Nandakumar *et al.* synthesized a ZnO hydrogel for psaAWH and simulated the binding energy of water molecules in the pore using theoretical calculations<sup>[114]</sup>. The DFT results indicate that a high binding energy exists between water molecules and materials at the initial stage of water adsorption, which corresponds to the strong interaction (chemical absorption/hydroxylation) between water molecules and hydrophilic sites during nucleation. With the continuous adsorption of water molecules, the binding energy decreases sharply, which corresponds to the physical adsorption process of multilayer adsorption and the capillary condensation

stage. When hygroscopic salt is incorporated into the hydrogel, the mechanism primarily involves water vapor adsorption driven by the deliquescence of salt. In this case, water is captured by the formation of crystalline water, salt dissolution, and solution adsorption, and the polymer pores generally serve as storage space for water molecules<sup>[112]</sup>. The water adsorption process of the hygroscopic polymer is summarized in [Figure 11](#), and desorption is the reverse process.

Considering their high water adsorption capacity, although hygroscopic polymers do not display S-type water vapor adsorption isotherms, they have been used in psaAWH in recent years, and promising results have been obtained<sup>[115-121]</sup>. Nandakumar *et al.* synthesized a solar-driven ZnO hydrogel for water-vapor harvesting under high relative humidity (90% RH)<sup>[114]</sup>. Separately, Ni *et al.* achieved high water production (*c.a.* 4.57 kg m<sup>-2</sup> day<sup>-1</sup>) under 90% RH and sunlight exposure by introducing photothermal segments into an integrated hygroscopic photothermal organogel (POG) [[Figure 12A](#)]<sup>[122]</sup>. Moreover, incorporating segments with LCST in hygroscopic polymers can accelerate the release of water molecules and improve water production<sup>[37,116,121]</sup>. For example, Zhao *et al.* demonstrated the release of liquid water from a hydrogel through a photoresponse effect [[Figure 12B](#)]<sup>[116]</sup>. When the ambient temperature is lower than LCST, the hydrogel shows hydrophilicity and can adsorb a large number of water molecules in the framework. As the temperature rises above LCST, the poly(N-isopropylacrylamide) (poly-NIPAM) segment in the hydrogel becomes hydrophobic, resulting in the rapid release of water molecules from the hydrogel in liquid form. To further improve the water adsorption capacity, hygroscopic salts are commonly introduced into polymers<sup>[123-127]</sup>. For example, Lei *et al.* synthesized a LiCl-doped zwitterionic hygroscopic polymer<sup>[118]</sup>. The water uptake of the polymer was enhanced and finally showed excellent water production (5.87 L kg<sup>-1</sup> day<sup>-1</sup>).

Owing to their macroporous inner structure and rich active groups inside hygroscopic polymers, they can adsorb and filter pollutants in the atmosphere during psaAWH application<sup>[128]</sup>. Yao *et al.* synthesized a porous sodium polyacrylate/graphene framework (PGF) that can capture atmospheric water contaminated by harmful substances and release clean water<sup>[129]</sup>. The abundant active groups of the hygroscopic polymers make them tunable. After the incorporation of LiCl and MOF-101, owing to the synergistic effects of space pressure from the rigid polymer chain and strong water affinity, active and continuous water production is finally realized<sup>[28]</sup>. Although hygroscopic polymers have been widely used in psaAWH, most function optimally at higher RH because of the lack of S-type water adsorption isotherms and display volume swelling after water absorption. Although some hydrogels offer higher water uptake at low RH by doping with hygroscopic salts, such as CaCl<sub>2</sub> and LiCl, etc, the salts may remain in the collected water, making it unfit for consumption.

### Crystalline porous organic salts

CPOs are emerging crystalline porous materials composed of organic acids and organic bases formed through hydrogen bond-assisted ion bond interactions<sup>[130]</sup>. Compared to hydrogen-bonded organic frameworks (HOFs), CPOs frameworks possess both hydrogen and ionic bonds. These bonds support channels with both high polarity and regularly distribute positive and negative charges from organic acids and bases<sup>[130,131]</sup>. These charged and highly polar channels impart CPOs with excellent properties compared with other porous materials<sup>[132-138]</sup>. Owing to the strong ionic bond interactions in the framework, most CPOs exhibit good water stability. For example, CPOS-2 shows high proton conductivity and crystallinity under high relative humidity (98% RH) and temperature (60 °C)<sup>[138]</sup>. Because the pore size of CPOs is generally small, capillary condensation does not occur during the adsorption of water vapor; therefore, the adsorption mechanism of CPOs is mainly cluster adsorption. The adsorption/desorption process of the CPOs in psaAWH can be described in [Figure 7B](#), and the detailed process is discussed below.

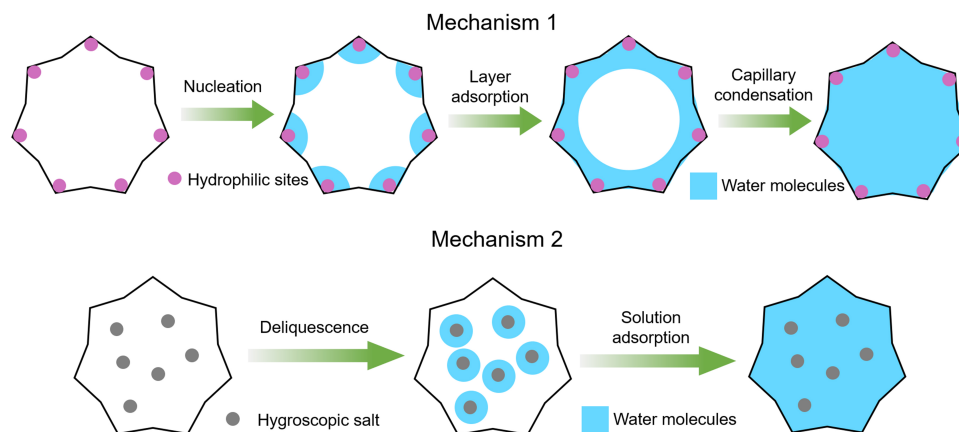


**Figure 11.** The adsorption process of water by hygroscopic polymers.

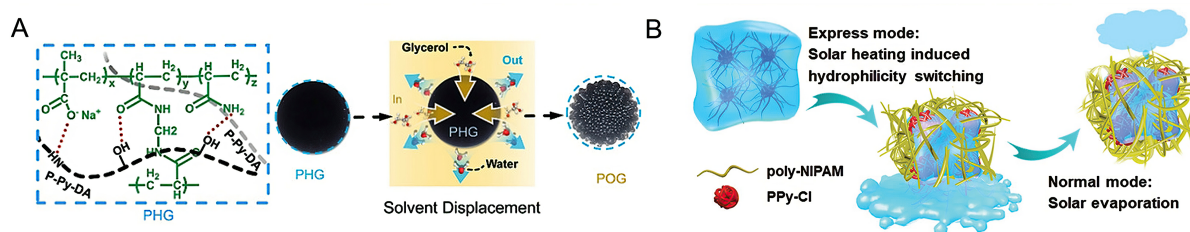


**Figure 12.** (A) Structure of a photothermal organogel (POG) and its synthesis process diagram. Reproduced with permission<sup>[122]</sup>. Copyright John Wiley and Sons; (B) schematic illustration of express mode and normal mode for water release powered by solar energy. Reproduced with permission<sup>[116]</sup>. Copyright John Wiley and Sons.

Zhang *et al.* synthesized CPOS (CPOS-6) containing strong organic acids (tetrakis(4-sulfophenyl) methane, TSPM) and bases (tetrakis(4-amidinophenyl) methane, TAmPM)<sup>[29]</sup>. The unique double-layer water adsorption process of CPOS-6 afforded rapid water adsorption and release kinetics, leading to a high expected water production ( $2.16 \text{ g g}^{-1} \text{ day}^{-1}$ ). In this double-layer adsorption process, the first layer of water molecules adsorbed by the strong polar groups acts as a binding site for the second layer of adsorption, which improves the second layer adsorption rate [Figure 13]. Furthermore, weak hydrogen bonds in the second layer of adsorbed water molecules were readily desorbed during desorption. Although the applications of CPOSs in psAWH remain nascent, their unique advantages of highly polar pores make them promising for psAWH. Moreover, CPOSs can be readily synthesized at ambient temperature and pressure, thereby simplifying industrial production. However, the water uptake should be improved.

### Porous carbon

Porous carbon has been used in various fields because of its ultrahigh thermal and chemical stability and high functionalizable porosity<sup>[139]</sup>. Accordingly, their water adsorption performance has been widely studied<sup>[140-143]</sup>. Depending on the pore structure, activated carbon, an archetypical classic porous carbon material, can adsorb water via capillary action<sup>[144]</sup>. The water vapor adsorption of porous carbon primarily involves the following processes<sup>[144]</sup>: nucleation, water cluster growth, and pore filling [Figure 14]. In porous carbon, the nucleation sites can be ultramicroporous, defective, or hydrophilic groups. This process can cause the water vapor adsorption isotherm to exhibit a steep water uptake under varying low RH. If the affinity of the hydrophilic sites is weak, the inflection point of steep water uptake will move appropriately to a high RH. After nucleation, it is followed by the growth and coalescence of water clusters, in which pore

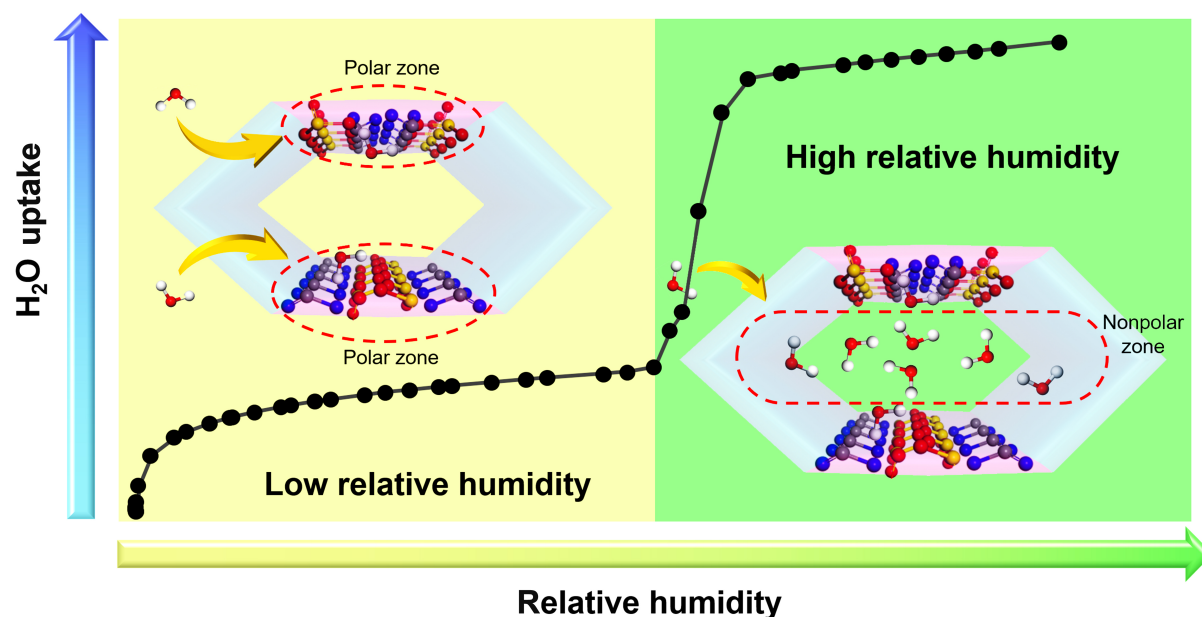


**Figure 13.** Schematic of water adsorption on CPOS-6 featuring a double hydrogen bond system under different humidity conditions. Reproduced with permission<sup>[29]</sup>. Copyright John Wiley and Sons.

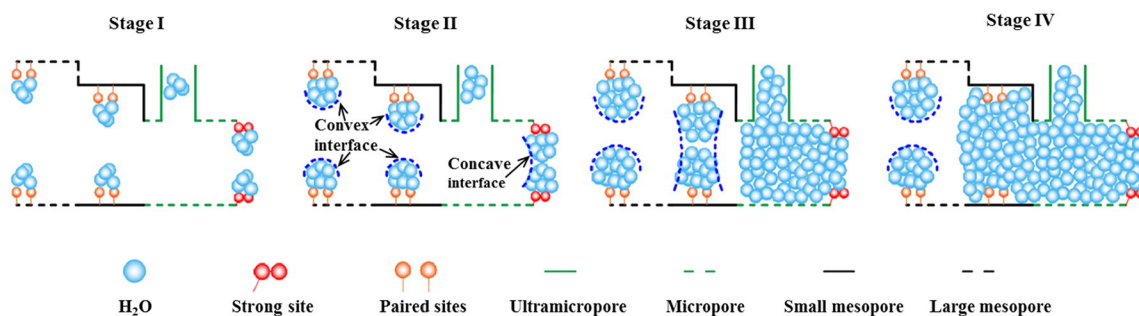


**Figure 14.** Schematic description of water adsorption in porous carbon, stage I-IV: cluster formation, cluster growth and coalescence, micropore filling and mesopore filling. Reproduced with permission<sup>[144]</sup>. Copyright Elsevier.

filling can occur rapidly if the distance between the hydrophilic sites is small, and the second step water uptake appears in the water vapor adsorption isotherm. In contrast, if the distance between the hydrophilic sites is large, pore filling will not occur immediately, and the second step water uptake can only occur by increasing the RH. The last step is the pore-filling stage, in which microporous filling occurs before  $RH < 60\%$ , followed by mesoporous filling.

To date, porous carbon materials have been successfully used as adsorbents for psaAWH<sup>[145-149]</sup>. For example, Byun *et al.* synthesized epoxy-functionalized porous carbon featuring a maximum water uptake (39.2-42.4 wt%) at reasonable temperatures (5-45 °C), which can be regenerated at a relatively mild temperature (55 °C)<sup>[150]</sup>. Recently, Song *et al.* synthesized porous carbon with rapid water adsorption/desorption kinetics owing to the existence of fast water transmission channels in the material [Figure 15]<sup>[151]</sup>. Finally, the porous carbon obtained a water production of  $0.18 \text{ L kg}_{\text{Carbon}}^{-1} \text{ h}^{-1}$  under 30% RH. Thus far, porous carbon has remained a competitive adsorbent material for psaAWH because of its stability and other advantages. However, the water uptake of porous carbon applied to psaAWH is still low, and the problem of improving its water adsorption needs to be resolved.

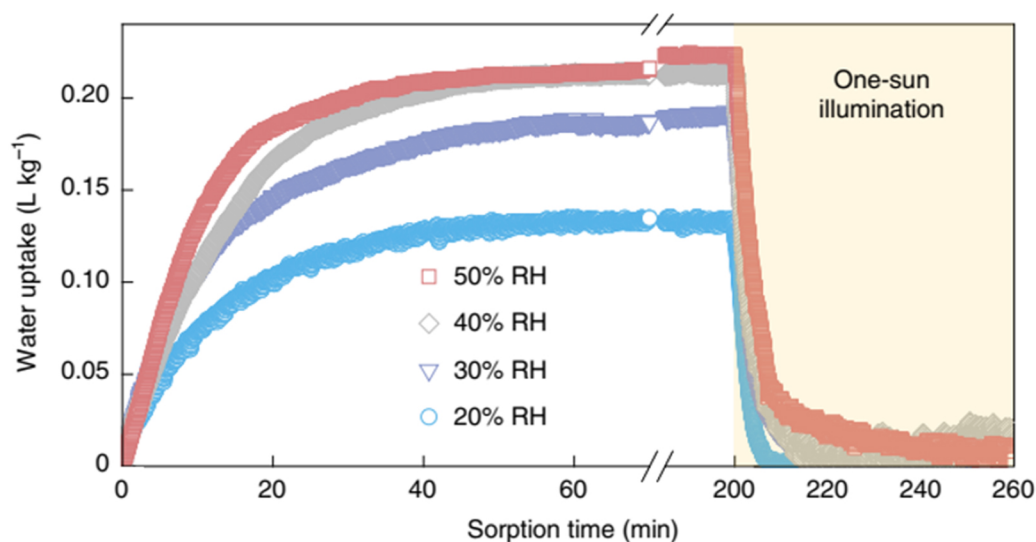


**Figure 15.** Water adsorption/desorption tests at 25 °C and 20%-50% RH for Steam-80. At 200 min, the sample is exposed to one-sun irradiation to release the water. Reproduced with permission<sup>[151]</sup>. Copyright Springer Nature.

In this section, we introduce the adsorbents applied to psaAWH and their respective adsorption and desorption mechanisms, as well as some examples of their applications. Based on the advantages and disadvantages of each material mentioned in each section, we think that MOFs and hydrogels may be the closest materials to commercialization at present, owing to their designability, high water adsorption capacity, and good stability. However, the two materials still have their own limitations, such as the uncertain toxicity of MOFs and the low water uptake of hydrogels at low RH. To visually compare the psaAWH performance of the different materials, the psaAWH-related properties of some typical adsorbents are summarized in [Table 2](#).

## INFLUENCE OF INHERENT PROPERTIES OF ADSORBENT ON WATER HARVESTING

### Effect of functional group

The functional groups in the adsorbent pores have a significant impact on psaAWH performance<sup>[78,149,150]</sup>. First, as described in greater detail in the next section, the introduction of functional groups into the adsorbent channels can tune hydrophilicity, thereby affecting the adsorption/desorption kinetics. Herein, we primarily focus on the effect of introducing functional groups on the water vapor adsorption isotherms of porous adsorbents. In 2014, Furukawa *et al.* compared a series of water vapor adsorption isotherms of Zr-containing MOFs and found that the introduction of hydrophilic groups into the pores altered the adsorption isotherms, affecting the psaAWH performance<sup>[19]</sup>. Recently, they synthesized a new MOF (MOF-333) with a strong hydrophilic linker (1-H-pyrazole-3,5-dicarboxylate, H<sub>2</sub>PZDC) of MOF-303 replaced by a weaker hydrophilic linker (2,4-furandicarboxylate, H<sub>2</sub>FDC). Subsequently, the authors obtained a series of isorecticular MOFs by modulating the ratio of these two linkers in the MOF framework and studied their water adsorption vapor isotherms [[Figure 16A](#)]<sup>[79]</sup>. With increasing weakly hydrophilic H<sub>2</sub>FDC content, the inflection pressure of the S-type water vapor adsorption isotherm gradually increased, which means a higher applied RH. In addition, the regeneration temperature of the adsorbent was reduced by 10 °C at the same RH due to the change of inflection pressure of water vapor adsorption isotherm, which reduced the energy consumption of psaAWH.

**Table 2.** psaAWH related properties of some typical adsorbents

Type	Materials	Adsorption process Water uptake (RH), adsorption time	Desorption process Desorption temperature, water release, desorption time	Ref.
Classic adsorbents	Silica	0.4 g g <sup>-1</sup> (75%), -	100 °C, -0.4 g g <sup>-1</sup> , -	[40]
	SAPO-34	0.3 g g <sup>-1</sup> (40%), 80 min	120 °C, 0.3 g g <sup>-1</sup> , 10 min	[91]
	Zeolite 13X	0.3 g g <sup>-1</sup> (40%), 60 min	120 °C, 0.2 g g <sup>-1</sup> , 20 min	[91]
MOFs	MOF-801	0.2 g g <sup>-1</sup> (30%), 200 min	85 °C, 0.2 g g <sup>-1</sup> , 30 min	[34]
	MOF-303	0.4 g g <sup>-1</sup> (40%), 80 min	85 °C, 0.4 g g <sup>-1</sup> , 40 min	[91]
	Al-fumarate	0.4 g g <sup>-1</sup> (40%), 150 min	65 °C, 0.4 g g <sup>-1</sup> , 20 min	[91]
	MOF-303/333	0.4 g g <sup>-1</sup> (40%), -	85 °C, 0.4 g g <sup>-1</sup> , one adsorption/desorption cycle 75 min	[79]
COFs	Cu-AD-SA MOF	0.15 g g <sup>-1</sup> (20%), 160 min	85 °C, 0.15 g g <sup>-1</sup> , -	[92]
	MIL-101 (Cr)@LiCl	0.77 g g <sup>-1</sup> (30%), 240 min	83 °C, 0.6 g g <sup>-1</sup> , 90 min	[83]
	COF-432	0.23 g g <sup>-1</sup> (40%), -	35 °C, 0.23 g g <sup>-1</sup> , -	[27]
Hygroscopic polymers	COF-480-hydrazide	0.35 g g <sup>-1</sup> (40%), -	85 °C, 0.33 g g <sup>-1</sup> , -	[110]
	PNIPAAM/Alg IPN gel	0.89 g g <sup>-1</sup> (90%), -	50 °C, 0.7 g g <sup>-1</sup> , -	[37]
	Super moisture-absorbent gel (SMAG)	2 g g <sup>-1</sup> (75%), 50 min	Sunlight, 2 g g <sup>-1</sup> , 10 min	[116]
	ZnO hydrogel	-0.6 g g <sup>-1</sup> (90%), 45 min	Sunlight, 0.6 g g <sup>-1</sup> , 15 min	[114]
CPOs	POG	6 kg m <sup>-2</sup> (90%), 12 h	Sunlight, 5.5 kg m <sup>-2</sup> , 700 min	[122]
	SHPFs	-0.6 g g <sup>-1</sup> (30%), 30 min	60 °C, -0.6 g g <sup>-1</sup> , 30 min	[152]
	CPOS-6	0.23 g g <sup>-1</sup> (70%), 52 min	40 °C, 0.12 g g <sup>-1</sup> , 30 min	[29]
Porous carbon	Steam-80	0.21 g g <sup>-1</sup> (26%), 45 min	Sunlight, 0.16 g g <sup>-1</sup> , 15 min	[151]

COFs: Covalent organic frameworks; CPOs: crystalline porous organic salts; MOFs: metal-organic frameworks; POG: photothermal organogel; RH: relative humidity; SHPFs: super hygroscopic polymer films.

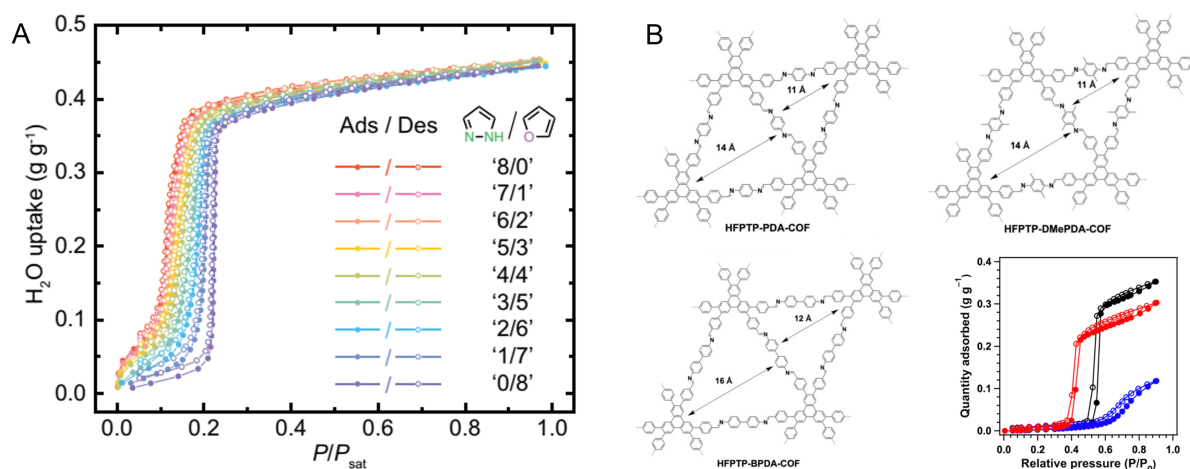


**Figure 16.** (A) Water sorption analyses on the multivariate MOF series at 298 K. Reproduced with permission<sup>[79]</sup>. Copyright The American Association for the Advancement of Science; (B) structures and water vapor adsorption isotherms at 298 K of HFFTP-PDA-COF (red), HFFTP-DMePDA-COF (blue) and HFFTP-BPDA-COF (black). Reproduced with permission<sup>[100]</sup>. Copyright Springer Nature.

Although the adsorbent applied RH and regeneration temperature can be reduced by increasing the hydrophobicity of the channel, excessive hydrophobicity may be detrimental to its psaAWH performance. As shown in [Figure 16B](#), the introduction of a hydrophobic methyl group not only results in the loss of the S-type water adsorption isotherm but also leads to a reduction in the water adsorption capacity<sup>[100]</sup>. In

addition, the functionality of the metal sites may also influence the adsorbent properties<sup>[153]</sup>. Rieth *et al.* modulated the inflection pressure of water vapor adsorption isotherm of MOFs through cation exchange and obtained a series of MOFs with different psaAWH performances<sup>[87]</sup>. For some macroporous adsorbents, such as hydrogels, the introduction of hydrophilic groups can enhance their water adsorption capacity at low relative humidity<sup>[129,148,154]</sup>. Zhao *et al.* synthesized a hydrogel crosslinked with a hygroscopic polymer that demonstrated enhanced water uptake ( $0.7 \text{ g g}^{-1}$ ) under 30% RH<sup>[116]</sup>. In addition, the combination of hygroscopic salts and the introduction of functional polymers can impart functionality and modulate the adsorbent psaAWH performance.

Generally, for the functional groups in the pore, the main influence is the applied RH range of psaAWH [Figure 17]. According to the climatic conditions of the area where psaAWH is to be implemented, the hydrophilicity of the adsorbent pores can be regulated to meet the requirements. In arid areas, the hydrophilicity of the pores can be increased. In contrast, in areas with high RH, we can reduce the hydrophilicity of the pores so that the inflection point ( $P_2$ ) is exactly the atmospheric RH [Figure 1B]. Therefore, the inflection point ( $P_1$ ) can be reached with minimal energy consumption, which significantly reduces energy consumption [Figure 16A]. In addition, we should pay attention to the change in water uptake caused by the functional groups in the pore [Figure 16B]. When modifying a pore with a functional group, significantly reducing the hydrophilicity of the channel should be avoided, which will lead to a significant decrease in water uptake.

### Effect of pore size

The adsorbent pore size has a considerable influence on the adsorbent psaAWH performance. First, it shows obvious effects on the water molecule transport kinetics. Intuitively, a larger pore size would improve the mobility of water molecules within the material; this hypothesis is considered in detail in the next section. However, a larger pore size does not necessarily result in a better adsorbent. For some crystalline materials such as MOFs, large pore sizes tend to result in poor water and structural stability, as rationalized by the theory of reticular chemistry, rendering them unsuitable for psaAWH<sup>[155]</sup>. In addition, for some macroporous adsorbents that rely on adsorption sites for water uptake, the number of active sites per unit volume is lower for larger pore sizes. Accordingly, they exhibited slower water adsorption rates than the corresponding microporous materials. This phenomenon has also been observed in some macroporous hydrogels<sup>[2]</sup>.

The adsorbent pore size may also influence the applicable RH range for the psaAWH by shaping the water vapor adsorption isotherm. For example, Abtab *et al.* synthesized a large-pore MOF (pore diameter = 1.7 nm), and the inflection point of its S-type water vapor adsorption isotherm was 60% RH [Figure 18A], which is higher than that of some small-pore MOFs (MOF-801, UiO-66, etc.)<sup>[85]</sup>. Therefore, it can only be used in an environment with humidity above 60%. Other materials with large pores, such as MIL-101<sup>[83]</sup>, PIZOF-2<sup>[19]</sup>, MOF-806<sup>[19]</sup>, and COF-670-hydrazine<sup>[110]</sup>, also demonstrate this behavior. Although the effects of pore size on the water adsorption curves of these 3D materials are apparent, the complexity of the interconnected channels of 3D porous materials complicates the mechanistic evaluation. In contrast, for 2D porous materials, the effect of the pore size on the water vapor adsorption isotherm is clear.

Gilmanova *et al.* synthesized two types of isorecticular 2D COFs (DUT-175 and DUT-176) and studied the effect of the pore size on water adsorption<sup>[107]</sup>. Figure 18B shows that both COFs possess one-dimensional channels with different pore sizes (16.4–25.7 and 21.9–31.8 Å, respectively). The larger pore size of DUT-176 resulted in a water vapor adsorption isotherm with a higher pressure inflection point (60% RH) relative to DUT-175. Similarly, two 2D COFs synthesized by Nguyen *et al.* also demonstrated this phenomenon<sup>[110]</sup>.

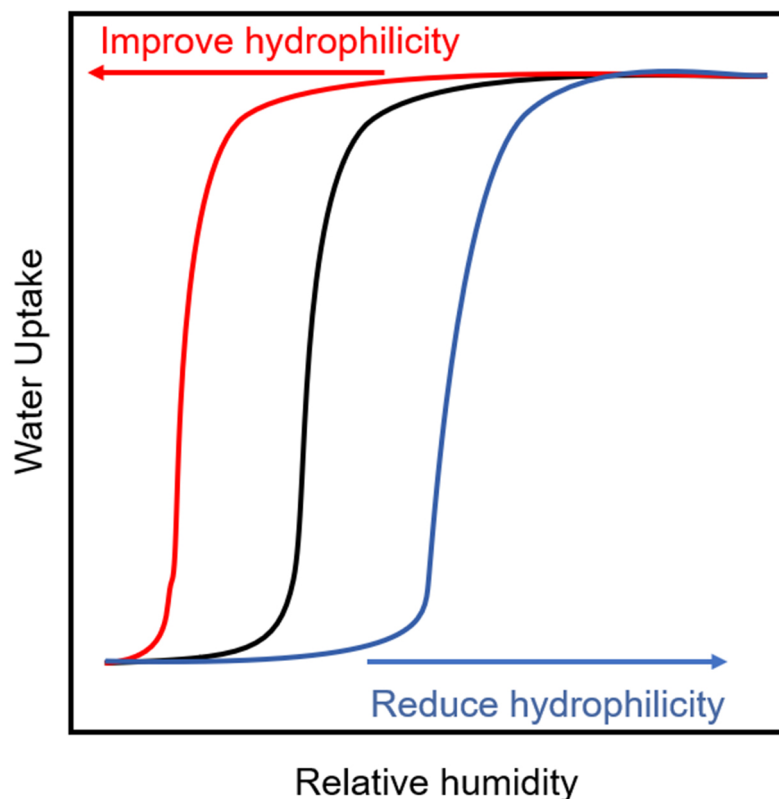


**Figure 17.** Influence of hydrophilicity of adsorbent pore on its applied RH.

Tan *et al.* studied the water cluster and adsorption processes of isorecticular 2D COFs [Figure 16B] and explained why larger pore sizes delayed steep water uptake<sup>[100]</sup>. Compared to small pores, larger pore sizes increase the hydrophobicity of the pores, thus reducing the channel confinement effect on water molecules. Therefore, a higher water vapor pressure (*i.e.*, high relative humidity) is required for steep water uptake. Although the water adsorption isotherm can be modulated by changing the pore size, the effect of pore size becomes less clear at sufficiently small pore sizes (*c.a.* < 1.5 nm). In addition, when the pore size increases to tens or hundreds of nanometers, the S-shaped adsorption isotherm may gradually transform into a type-III adsorption isotherm, which is not suitable for psaAWH. This type of water vapor isotherm is usually observed for most macroporous polymers.

Finally, changes in the adsorbent pore size may improve the water uptake and, therefore, the psaAWH performance. In fact, pore size affects water uptake by changing the pore volume of the adsorbent. Sometimes, increased pore size increases the pore volume and adsorption capacity of water molecules. Isorecticular framework expansion is an effective method for improving pore size<sup>[19,52]</sup> and has led to improved water uptake in HFPTP-PDA-COF and HFPTP-BPDA-COF [Figure 16B]. However, the increase in pore size may increase the channel hydrophobicity in some instances, thereby decreasing the water uptake<sup>[76,107]</sup>. In addition, the adsorbent water uptake may also be increased by building a hollow shell and hierarchical structure to provide large pores<sup>[84]</sup>. For example, Hu *et al.* prepared hollow MIL-101(Cr), which showed an enhanced water storage capacity and uptake owing to the high water storage capacity of the hollow part [Figure 19A]<sup>[156]</sup>. Finally, some adsorbents may swell due to water adsorption, resulting in a gradual increase in pore size and eventually reaching a very high water uptake. This phenomenon was observed in most of the hydrogels [Figure 19B]<sup>[121]</sup>.

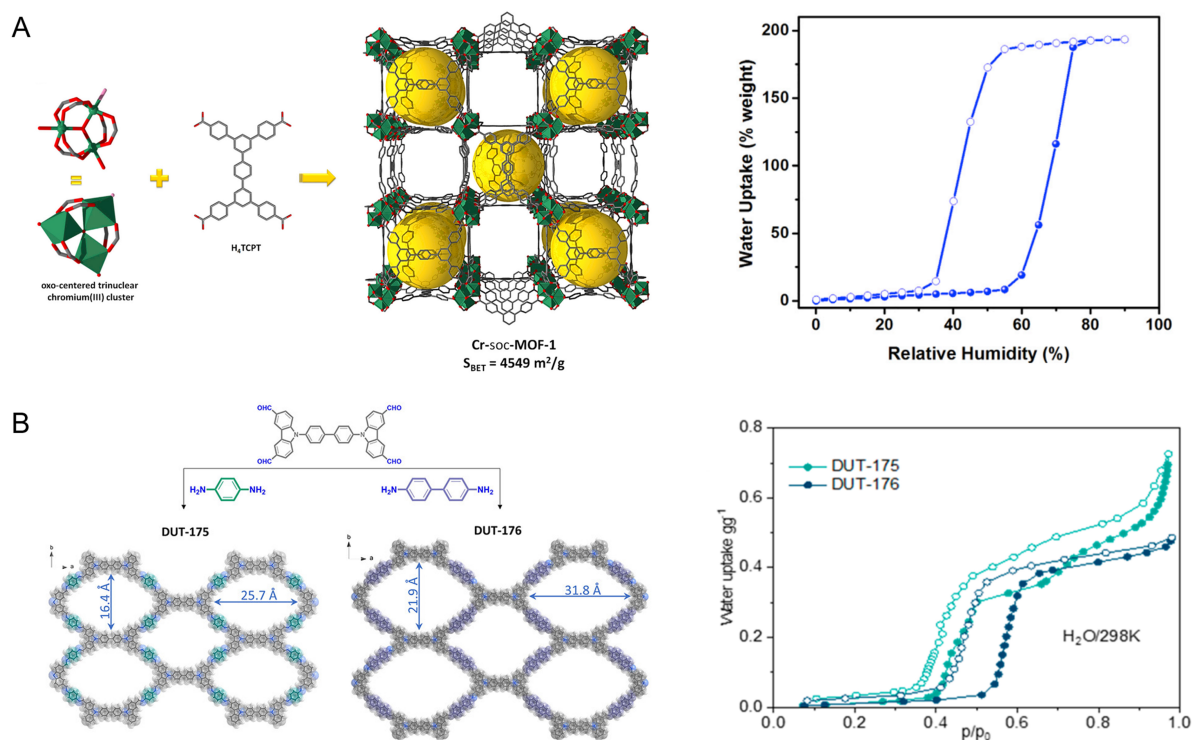


**Figure 18.** (A) Crystal structure and water vapor adsorption isotherm at 298 K of Cr-soc-MOF-1. Reproduced with permission<sup>[85]</sup>. Copyright Elsevier; (B) structure and water vapor adsorption isotherm at 298 K of DUT-175 and DUT-176. Reproduced with permission<sup>[107]</sup>. Copyright American Chemical Society.

In summary, by adjusting the pore size of the adsorbent, the psaAWH performance of the adsorbent can be controlled. In addition to grafting functional groups into the pores, we can also regulate the applied RH of the adsorbent by changing the pore size. In fact, the essence of the effect of pore size on the applied RH of the adsorbent is to change the hydrophilicity of the pores. In addition, to obtain high water uptake, a large pore size is beneficial, but as discussed, the applied RH of the adsorbent must be considered for practical applications. Therefore, increasing the pore size while satisfying the applied RH is the correct strategy to improve the psaAWH performance of the adsorbent. Besides, when increasing the pore size, we should also consider the hydrophobicity of the pore. If the hydrophobicity is too strong, it may lead to the reduction of water uptake.

### Surface area and crosslinking density

As an important property of porous materials, the surface area represents the total area of the internal and external surfaces on which porous materials can be used. In general, most active sites of porous materials are located on their surfaces; therefore, a large surface area can provide more active sites. Thus, the surface area has a significant influence on various properties of porous materials. The specific surface area (i.e., the total surface area per unit mass of the material) is generally used in porous materials. First, the specific surface area may affect the water uptake of the adsorbent. For example, for some crystalline porous materials (such as MOFs and COFs), a larger specific surface area is often accompanied by higher water uptake [Figure 16B, 18A]<sup>[79,85]</sup>. This is because in crystalline porous materials (MOFs and COFs), in addition to avoiding multiple interpenetrations and using new topology, the specific surface area is often improved by increasing the pore size, particularly for microporous materials. However, for mesoporous and macroporous materials, no correlation generally exists between the specific surface area and water

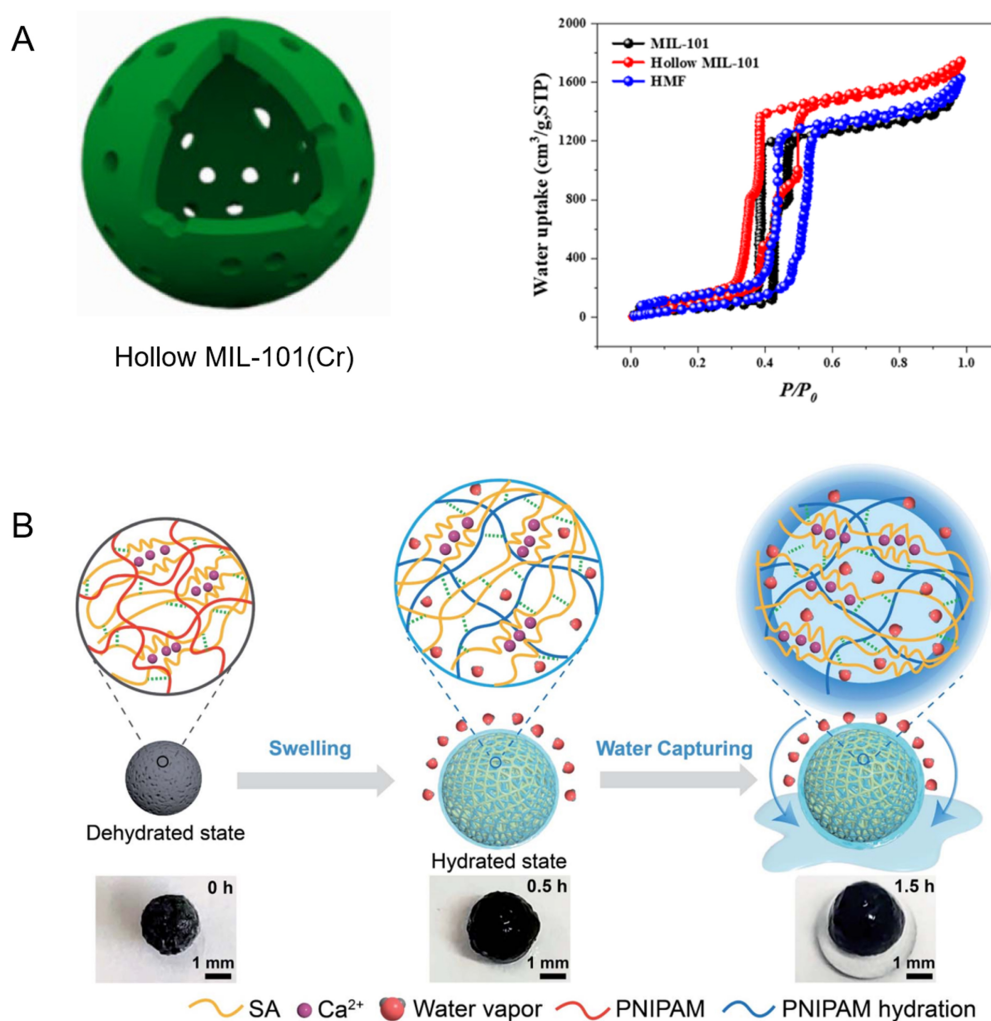


**Figure 19.** (A) Hollow MIL-101(Cr) and its water adsorption isotherm at 298 K. Reproduced with permission<sup>[156]</sup>. Copyright American Chemical Society; (B) hydrogel water absorption and swelling. Reproduced with permission<sup>[121]</sup>. Copyright Royal Society of Chemistry.

uptake<sup>[107,156]</sup>. The water uptake of the adsorbent was primarily determined by its pore volume. Thus, hydrogels have a small surface area but a large water uptake. Second, the specific surface area can affect the adsorption rate of water molecules. A large specific surface area often implies more accessible active surfaces, which can accelerate the nucleation and cluster/layer growth rate in the process of water molecule adsorption<sup>[113]</sup>. Nandakumar *et al.* prepared a zinc oxide hydrogel with large-area porous wrinkles, which showed a high water adsorption capacity<sup>[114]</sup>. By regulating the surface roughness and wrinkle degree, they obtained hydrogels with different specific surface areas and studied their water vapor adsorption rates [Figure 20A]. When the specific surface area is  $350 \text{ m}^2 \text{ g}^{-1}$ , the water uptake of the hydrogel can reach  $3.6 \text{ g g}^{-1}$  within 12 h, indicating a steep water vapor adsorption curve. With a decrease in the specific surface area, the water uptake of the hydrogel in 12 h gradually decreased, and the water vapor adsorption curve also gradually flattened, showing a slow adsorption rate.

The crosslinking density refers to the degree of crosslinking of the polymer chain, which has an important impact on the performance of the polymer. This affects the mechanical strength of the polymer. Appropriately increasing the crosslinking density can improve the structural stability of the material and

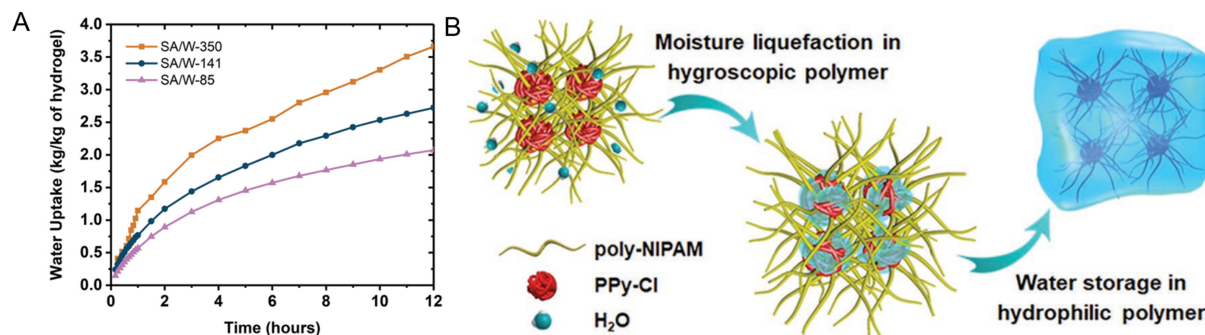


**Figure 20.** (A) Adsorption rates for different surface area to mass of the hydrogel ratios. Reproduced with permission<sup>[114]</sup>. Copyright John Wiley and Sons; (B) schematic illustration of the moisture absorption enabled by super moisture-absorbent gels (SMAGs). Reproduced with permission<sup>[116]</sup>. Copyright John Wiley and Sons.

contribute to enhancing the water adsorption/desorption cycle performance<sup>[157]</sup>. The crosslinking density also affected the swelling process of the hydrogels. Generally, a high crosslinking density tends to lead to a low swelling rate, which reduces the water adsorption capacity<sup>[158,159]</sup>. In addition, the adsorption of water molecules can be effectively controlled by regulating the crosslinking density of the polymer and other factors to improve the psaAWH performance of the adsorbent<sup>[112]</sup>. For example, Zhao *et al.* prepared a hydrogel (SMAG) with excellent moisture adsorption performance, which uses hygroscopic chloride-doped polypyrrole (PPy-Cl) clusters as a cross-linking point, and poly-NIPAM chains were inserted into the clusters to form an interpenetrating polymer network [Figure 20B]<sup>[116]</sup>. Therefore, the water adsorption performance of this hydrogel (SMAG) could be optimized by adjusting the crosslinking density.

Both the specific surface area and crosslinking density regulate adsorbent performance by affecting the interaction between the adsorbent and water molecules. The psaAWH performance of the adsorbent can be improved by properly designing these two properties. However, note that in some cases, the specific surface area and crosslinking density may have a negative impact on the water uptake of the adsorbent; therefore, it is necessary to modify the adsorbent reasonably to obtain the best performance.

## KINETICS PROCESS OF ADSORBENT

The water production of psaAWH is primarily determined by two factors. First, the high water uptake of the adsorbent implies that it can produce more water per adsorption/desorption cycle. Second, the fast cycling rates of the adsorbent (*i.e.* adsorption/desorption kinetics) can effectively increase the number of cycles of the adsorbent per unit time to obtain higher water production. The previous section discussed methods for improving the water uptake of adsorbents. This section discusses methods to improve the adsorption/desorption kinetics of the adsorbent.

To date, various effective methods for improving the adsorption/desorption kinetics of adsorbents have been developed. First, based on the adsorption mechanism of the adsorbent, the adsorption/desorption kinetics can be accelerated by proper modification of the adsorbent. Also, Taheri *et al.* proved that the active sites of biochar from pomegranate are the reason for its rapid adsorption kinetics at the initial stage of adsorption process<sup>[160]</sup>. As mentioned above, although the water vapor adsorption mechanism of various adsorbents is different, it can be generally classified into the following processes: nucleation, cluster/layer adsorption and pore filling. In this process, nucleation is a strong interaction between water molecules and hydrophilic sites in the pore, pore filling is a weak physical interaction, and cluster/layer adsorption is an intermediate state. Therefore, the kinetic process of nucleation and cluster/layer adsorption can be

effectively affected by regulating the hydrophilicity of the adsorbent. Wang *et al.* demonstrated AWH by grafting hydrophilic  $[\text{FeCl}_4]^-$ -doped poly(3,4-ethylenedioxythiophene) (PEDOT) microtubules onto the surface of a red brick<sup>[154]</sup>. These microtubules accelerate the nucleation and layer adsorption of water molecules on the surface of red bricks at ambient humidity and transport water molecules to the adsorbent interior through the porous network of red brick, thus accelerating the water harvesting rate [Figure 21]. Although hydrophilic modification can accelerate the adsorption kinetics, it increases the regeneration temperature of the adsorbent; therefore, it should be used reasonably according to the actual situation.

The transport speed of molecules improves with temperature increase. As reported by Messaoudi *et al.*, with the increase in temperature, the mobility of TZ molecule accelerates, which promotes the rapid absorption of TZ by adsorbent<sup>[161]</sup>. Therefore, increasing the desorption temperature of adsorbent can effectively speed up the desorption kinetics [Figure 22A]. Hanikel *et al.* used a solar power generation system to heat a MOF adsorbent, accelerating the water release rate, realizing multiple adsorption/desorption cycles in one day, and obtaining high water production ( $1.3 \text{ L kg}^{-1} \text{ day}^{-1}$ )<sup>[91]</sup>. However, direct heating relying on external factors not only consumes a significant amount of energy but also evades adsorbent material advancements. Various advances in adsorbent kinetics based on material design have been reported. The incorporation of photothermal materials into adsorbents to accelerate the release of water through sunlight irradiation has been reported. Wu *et al.* prepared a  $\text{T}_3\text{C}_2$  (a photothermal material)-incorporated MOF adsorbent (TUN/SA), which can increase to  $100 \text{ }^\circ\text{C}$  in 6 min under the irradiation of  $103 \text{ mW cm}^{-2}$  light, realizing the rapid release of water molecules. Compared to direct heating, the incorporation of photothermal materials can rapidly heat the adsorbent from the inside, resulting in rapid desorption kinetics [Figure 22B]<sup>[86]</sup>. However, the introduction of photothermal materials leads to a reduction in the adsorbent percentage per unit mass, and may block the pores of the adsorbent, thereby sacrificing a portion of the water adsorption capacity. In order to avoid this problem, we can reduce the amount of photothermal materials and make them disperse as evenly as possible, so that the adsorption performance of the adsorbent is less affected<sup>[162]</sup>.

According to previous reports<sup>[163]</sup>, there are three main processes for the adsorption of guest molecules by adsorbent: external diffusion; intra-particle distribution; adsorption on the active sites. For vapor adsorption of adsorbent, the intercrystalline diffusion also needs to be considered. External diffusion is mainly affected by the engineering of psaAWH devices, including the design of adsorbent bed and heating module. A more detailed overview of the engineering of psaAWH devices, including heat conduction and mass conduction, etc. can be found in Wang's article<sup>[162]</sup>. For adsorbent, the intra/inter-crystalline diffusion and adsorption on the active sites are the main factors affecting its kinetic process. The effect of active sites has been discussed above. The intracrystalline diffusion can be expressed by Fick's law<sup>[164]</sup>:

$$\frac{\partial C}{\partial t} = \frac{1}{r_c^2} \frac{\partial}{\partial r} \left( D_\mu r_c^2 \frac{\partial C}{\partial r} \right) \quad (1)$$

where  $C$  is the vapor concentration,  $t$  is the time,  $r_c$  is the spherical radius of the adsorbent, and  $D_\mu$  is the intracrystalline diffusivity of the vapor. However, the diffusivity in Eq. 1 varies with the temperature and vapor uptake; therefore, the characteristic intracrystalline diffusivity crystals are used to represent the average diffusivity within a certain range of temperature and vapor uptake. The following equation can be used to describe the average diffusion coefficient of vapor adsorption kinetics<sup>[162,164]</sup>:

$$\frac{\partial C_\mu}{\partial t} = \frac{15}{r_c^2} D_\mu (C_{eq} - C_\mu) \quad (2)$$

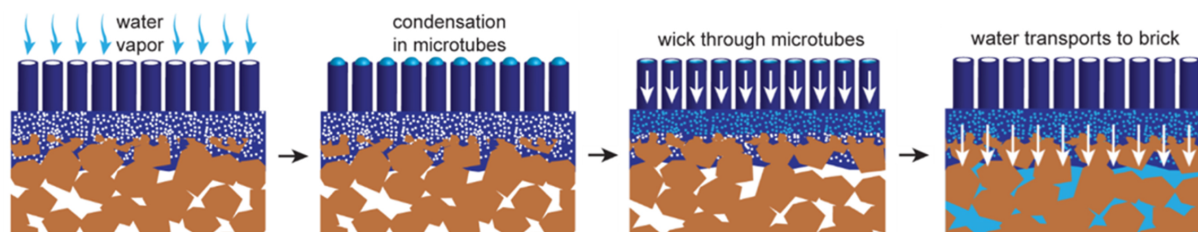


**Figure 21.** Water vapor transport from air to brick through PEDOT microtubes. Reproduced with permission<sup>[154]</sup>. Copyright American Chemical Society.

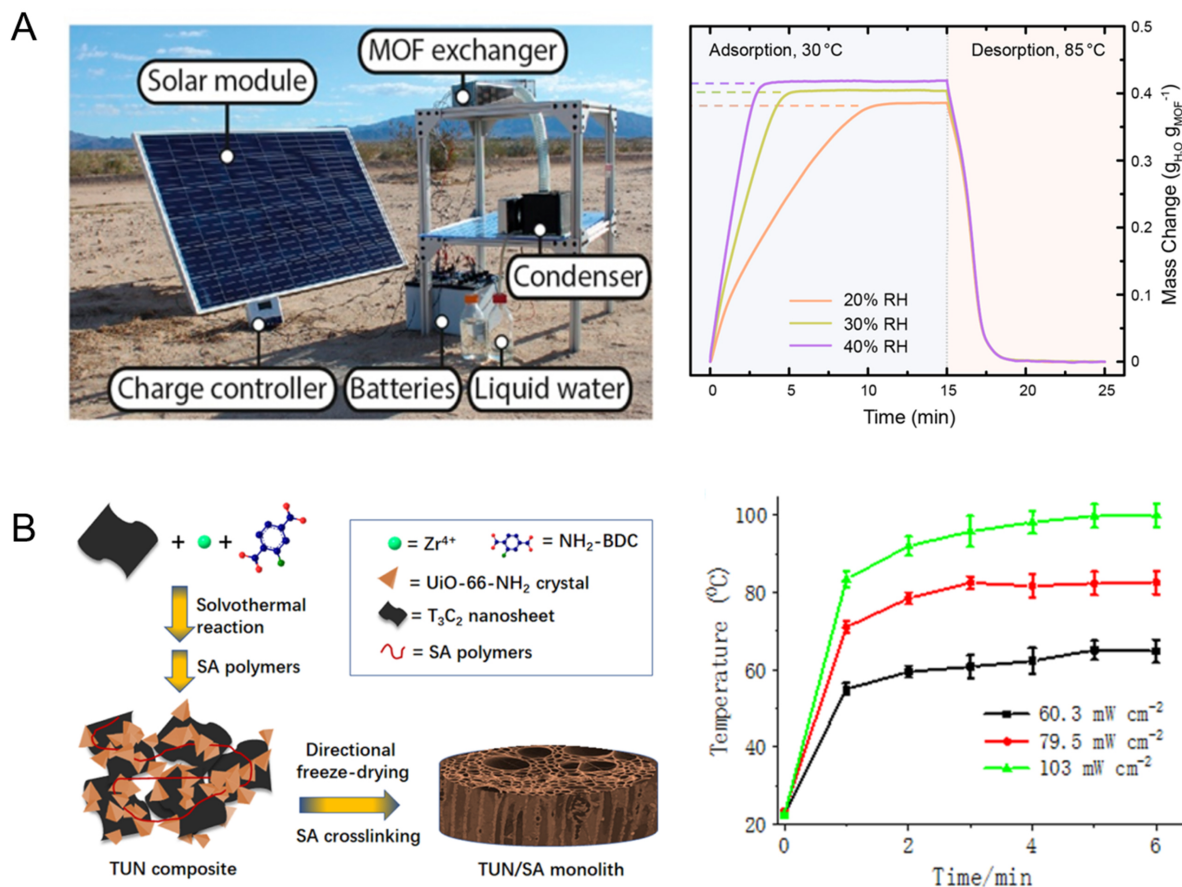


**Figure 22.** (A) Photograph of a psaAWH device and the adsorption/desorption kinetics of the adsorbent. Reproduced with permission<sup>[91]</sup>. Copyright American Chemical Society; (B) scheme of the preparation process for a photothermal TUN/SA adsorbent and its photothermal conversion performance. Reproduced with permission<sup>[86]</sup>. Copyright American Chemical Society.

where  $C_{\mu}$  is the instantaneous vapor concentration in the adsorbent at time  $t$ ;  $C_{eq}$  is the equilibrium vapor concentration in the adsorbent. As shown in Eq. 2, the smaller the size of the adsorbent, the faster the diffusion rate in the crystal. However, an extremely small adsorbent will hinder the intercrystalline diffusion of water vapor. Intercrystalline diffusion ( $D_V$ ) can be described by the following equation<sup>[164]</sup>:

$$D_V = \varepsilon^{3/2} \left( \frac{1}{D_{Vap}} + \frac{1}{D_K} \right)^{-1} \quad (3)$$

where  $D_{vap}$  is the diffusivity of vapor molecules in air,  $D_K$  is the Knudsen diffusivity, and  $\varepsilon$  is the porosity of the adsorbent packing layer, which is related to the size and geometry of the adsorbent. In general, a smaller size of the adsorbent implies a smaller value of  $\varepsilon$ . Besides, the adsorbent geometry can also affect the value of  $\varepsilon$ , but the relationship is complex. Therefore, psaAWH performance can be optimized by adjusting the size and geometry of the adsorbent.

As discussed, adsorbent size and geometry can affect its kinetic process by affecting the intra/inter-crystalline vapor diffusion<sup>[164]</sup>. A rapid kinetic rate was obtained using a reasonably designed adsorbent geometry. For example, Yilmaz *et al.* prepared a polymer-Au@MOF mixed-matrix material (PCA-MOF) featuring a cone array structure, which enabled the released water to rapidly accumulate at the cone tip and form droplets, thus accelerating intracrystalline diffusion<sup>[28]</sup>. It also enables rapid water separation from the adsorbent surface to accelerate the release of internal water [Figure 23A]. In addition, adsorbent films offer an increased contact area with the atmosphere and heater, resulting in a rapid kinetic process<sup>[152,165]</sup>. Guo *et al.* prepared super hygroscopic polymer films (SHPFs), which can undergo a transition from hydrophilic to hydrophobic after being heated. During the psaAWH process, SHPFs can be attached to a metal heating plate. Therefore, the rich porous structure and large heating area of the SHPFs enable rapid thermoresponsive hydrophobic transformations, leading to a rapid water release rate [Figure 23B]<sup>[152]</sup>.

In general, intracrystalline diffusivity is slower in adsorbents. The introduction of large pores in the adsorbent can be considered as a strategy to shorten the intracrystalline diffusion path, thus accelerating the kinetic process<sup>[84]</sup>. One approach is to build a shell structure in adsorbent that allows water molecules to freely diffuse inside, leading to rapid kinetics. Compared with MIL-101(Cr) powder, the hollow MIL-101(Cr) spheres showed faster adsorption kinetics because water molecules could reach the adsorption sites faster in the large cavity [Figure 19A]<sup>[156]</sup>. Rapid water transport through a hierarchical pore structure is another strategy for shortening the intracrystalline diffusion path<sup>[120,166,167]</sup>. Wang *et al.* prepared a nanostructured biopolymer hygroscopic aerogel (NBHA) that exhibited rapid water transport [Figure 24A]<sup>[127]</sup>. Under natural light irradiation, the water adsorbed in the aerogel can be quickly transported to the surface through the hierarchical pore structure, resulting in rapid regeneration. Xu *et al.* prepared an adsorbent with a vertically arranged channel [Figure 24B]<sup>[125]</sup>. During adsorption, water molecules may quickly diffuse to the interior of the adsorbent through the large pores to be adsorbed by the numerous active sites. In addition, this 1D channel minimizes the diffusion distances for water molecules between the interior and the surface of the adsorbent. Finally, these factors led to high water production ( $2.12 \text{ L kg}_{\text{adsorbent}}^{-1} \text{ day}^{-1}$ ).

Although the aforementioned strategies have achieved significant results in accelerating the adsorption kinetics, the intracrystalline diffusion rate, especially in micropores, has not been substantially improved. According to Wu's work<sup>[168]</sup>, the smaller the pore size of the adsorbent, the lower its applied RH. Therefore, accelerating the diffusion of vapor in the adsorbent micropores will greatly promote the development of psaAWH. Herein, the transport behavior of water molecules in the micropores is further re-examined from a new perspective (superfluidity).

Superfluidity, in which molecules or ions move collectively and directionally in confined channels, results in the rapid transport of matter<sup>[169]</sup>. The earliest report of superfluidity in 1938<sup>[170,171]</sup> was based on observations of this phenomenon in  $^4\text{He}$  below 2.17 K. When  $^4\text{He}$  passes through a channel with a diameter of less than 100 nm, its viscosity approaches zero, indicating that it can be transmitted in the channel at a superfast speed without energy loss. Subsequent studies have shown that the temperature at which the superfluidity phenomenon occurs can gradually increase with a decrease in the channel diameter<sup>[172]</sup>. In superfluidity,

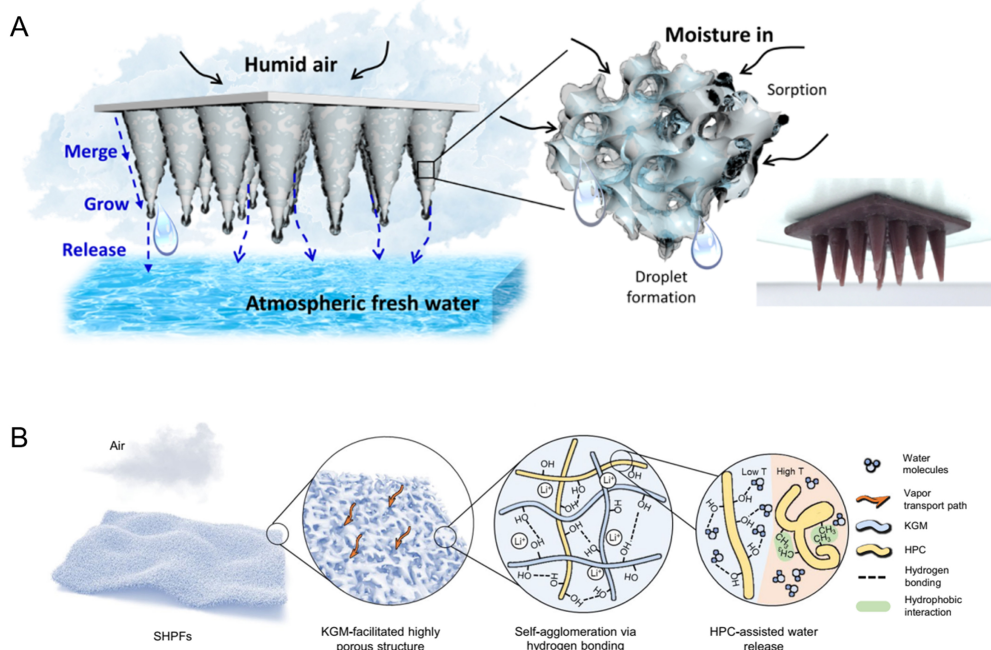


**Figure 23.** (A) Water release process of PCA-MOF cone array. Reproduced with permission<sup>[28]</sup>. Copyright The American Association for the Advancement of Science; (B) water adsorption and release processes of SHPFs. Reproduced with permission<sup>[152]</sup>. Copyright Springer Nature.

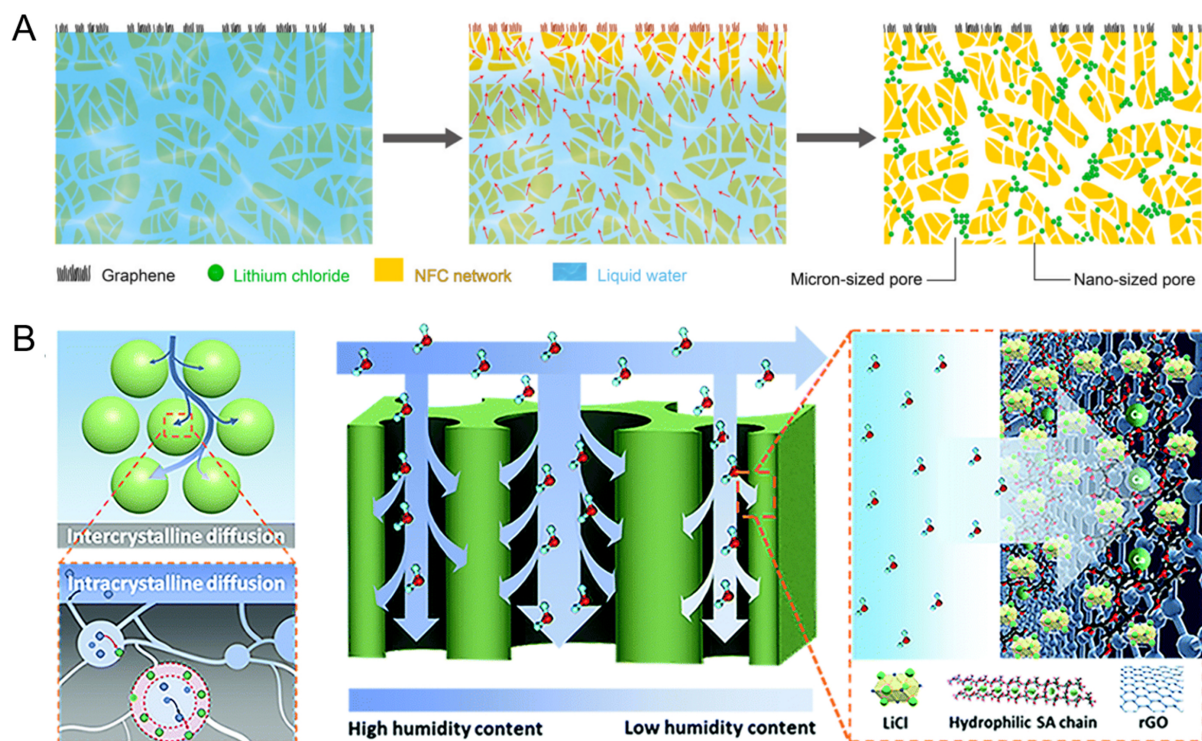


**Figure 24.** (A) Water vapor transport pathways of NBHA in solar-powered regeneration. Reproduced with permission<sup>[127]</sup>. Copyright Elsevier; (B) intercrystalline and intracrystalline diffusion of water vapor in the vertically aligned nanocomposite sorbent, and the scheme of water vapor transport pathways in the vertically aligned macropore. Reproduced with permission<sup>[125]</sup>. Copyright Royal Society of Chemistry.

particles move directionally in an ordered manner, and the driving force to form this state is the attraction-repulsion balance (*i.e.*, the lowest point of the potential energy)<sup>[173]</sup>. To achieve orderly motion, the attractive potential ( $E$ ) must be greater than the thermal noise ( $k_B T$ ), *i.e.*,  $E > k_B T$ <sup>[174]</sup>. For particles, the attractive potential ( $E$ ) can be described using the potential-distance curve [Figure 25]. As the particles approach each other, the attractive potential gradually decreases. When the distance is shortened to a certain value, the attractive potential reaches a minimum  $E_0$ , and the attraction between the particles is at a maximum. As the distance continues to decrease, the attractive potential gradually increases and eventually becomes positive, indicating that the particles begin to exhibit a repulsive force. According to Jiang's work<sup>[174]</sup>, the absolute value of  $E_0$  is approximately equal to the thermal noise at the critical temperature ( $T_C$ ) of the particles, *i.e.*,  $|E_0| \sim k_B T_C$ . Therefore, to achieve <sup>4</sup>He superfluidity, due to the low critical temperature of helium (5.20 K), the temperature must be reduced low enough ( $< 2.17$  K) to shorten the distance between the He atoms to ensure a high attractive potential ( $|E| > k_B T$ ).

As mentioned previously, the attractive potential ( $E$ ) must be greater than the thermal noise ( $k_B T$ ) for a superfluid to be formed. In addition to reducing the temperature required to reach this condition, superfluidity can be achieved through the space-confinement effect. On one hand, the confined space can reduce the degree of disorder of the particles; on the other hand, the confined space can help shorten the particle distance and make it easier to reach the lowest point of the potential energy ( $E_0$ ). Therefore, some molecules (such as water molecules) can exhibit superfluidity at room temperature in confined spaces<sup>[174]</sup>. As shown in Figure 26, when the channel size ( $D$ ) of the confined space is four times the vdW equilibrium distance ( $d_0$ ), superfluidity occurs in the middle of the channel. As the channel size decreases to  $\sim 2 d_0$ , all the molecules in the channel enter the lowest potential energy point, inducing molecular superfluidity.

Evidence of water molecule superfluidity has been found in artificial nanochannels. Wu *et al.* studied the transport of water molecules in carbon nanotubes (CNTs) and found that their flux was seven orders of magnitude larger than that of bulk water<sup>[175]</sup>. Molecular dynamics (MD) simulation showed that with a decrease in the size of the CNT channel (from 4.99 to 1.66 nm), the rate of water molecule transport increased significantly, and the proportion of ordered water molecules in the channel also increased gradually, indicating ordered fast transport of the water molecules. For psaAWH, the fast water transport behavior in the micropores shown by some materials may be related to superfluidity. For example, in the nanoconfined channel of CPOS-6, water in the weak adsorption layer undergoes weak hydrogen bonding interaction with the strong adsorption layer, ensuring that the channel has a moderate affinity to help reduce the disorder of the water molecules [Figure 27A]<sup>[29]</sup>. Consequently, it is possible to achieve rapid and orderly transport of the water molecules in the channel, leading to a fast kinetic process. Based on theoretical simulations, Song *et al.* controlled the hydrophilic group content and pore size in porous carbon<sup>[151]</sup>. In the theoretical calculations in this study, for a certain density of hydrophilic groups in porous carbon, the diffusion energy barrier of the water molecules increased with an increase in the number of hydrophilic groups [Figure 27B]. This may be due to the increased hydrophilicity, which strengthens the interaction between the pore and water molecules, thus destroying the orderly movement of the water molecules, thereby increasing the transmission energy barrier. From the above discussion, we can reasonably infer that water molecule superfluidity can exist in nanoconfined channels, thus promoting the rapid transport of water molecules. The formation of a superfluid is a feasible strategy for improving the intracrystalline diffusion of the psaAWH adsorbent.

## CONCLUSION AND OUTLOOK

In this review, we introduced the working principles and general processes of psaAWH. Compared with other freshwater production technologies, psaAWH has the advantages of a wide application range and no

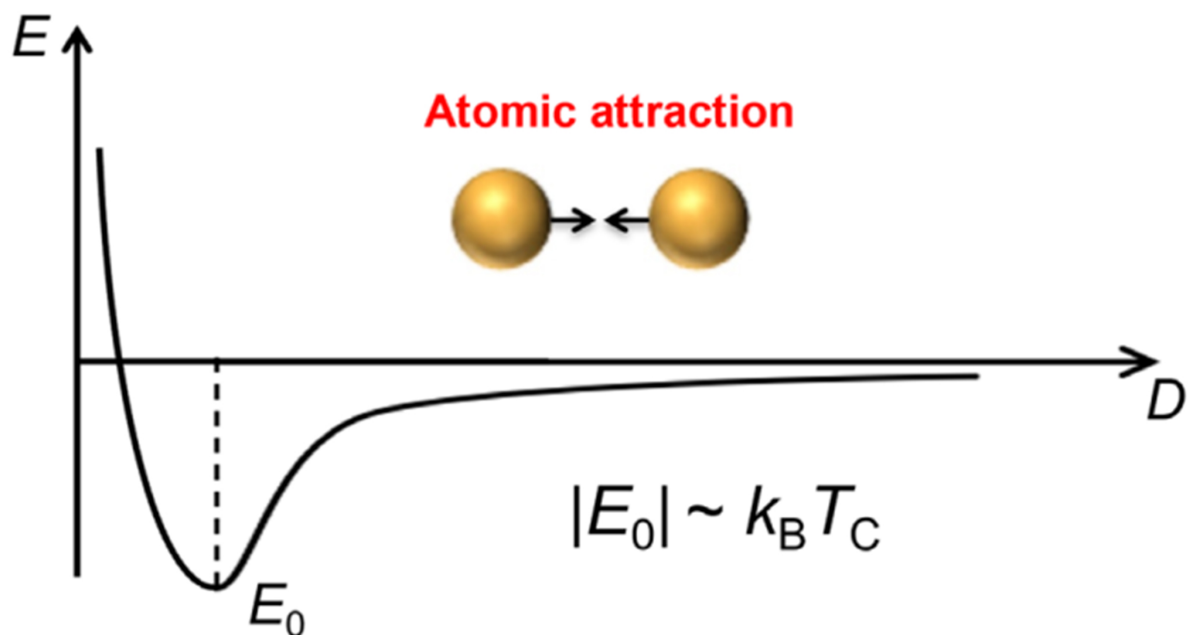


**Figure 25.** The potential-distance curve indicates the sufficient and necessary condition for the formation of an ordered structure of atoms. Reproduced with permission<sup>[174]</sup>. Copyright Chinese Chemical Society.

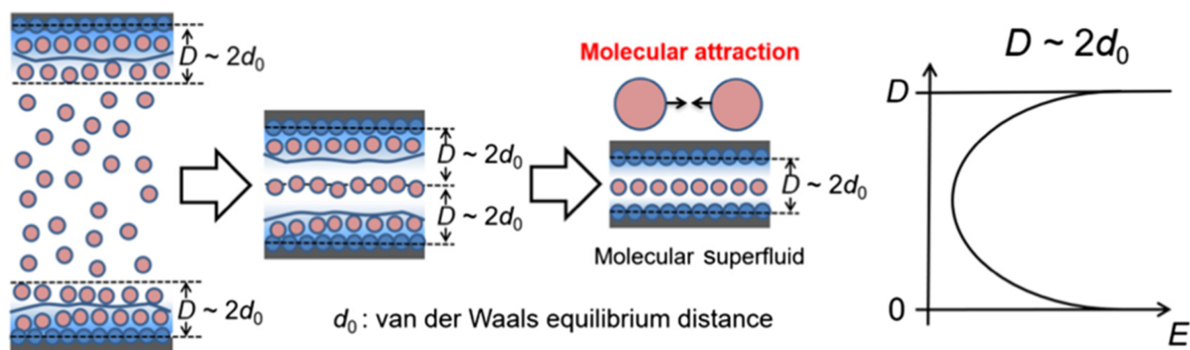


**Figure 26.** Occurrence of molecular superfluidity when the channel size of the confined space is reduced to  $2d_0$ . Reproduced with permission<sup>[174]</sup>. Copyright Chinese Chemical Society.

climate or geographical restrictions. Porous adsorbent materials used for psaAWH were systematically summarized. Based on the water vapor adsorption mechanism of each material, the corresponding water vapor adsorption/desorption process was presented, the advantages and disadvantages of each adsorbent were discussed, and their development status was reviewed. Compared with traditional porous adsorbents, emerging porous materials with unique properties exhibit excellent psaAWH performance. Although the performance and applicability of psaAWH have improved with the development of various adsorbents, the industrial application of psaAWH has not been fully realized, and only some patents related to psaAWH have been applied<sup>[176-178]</sup>. Table 3 lists the commercial application prospects of different materials. The term ‘uncertain toxicity’ in the table indicates that the constituent elements of the COFs and CPOSSs are non-toxic, but some synthetic monomers may be toxic to the human body or cells; therefore, their toxicity is still uncertain at present. As shown in Table 3, hydrogels are the most promising materials for commercial

**Table 3. Summary of commercial application prospects of various materials for psaAWH**

Material	Stability	Recyclability	Toxicity <sup>1</sup>	Large-scale production
Zeolites	High stability	high-temperature regeneration	Most are non-toxic	Already used for commercialization
MOFs	Meet the needs of psaAWH	Yes	Toxicity mainly comes from some metals	Can be large-scale produced
COFs	Meet the needs of psaAWH	Yes	uncertain	No
Hydrogels	Meet the needs of psaAWH	Yes	Most are non-toxic	Already used for commercialization
Porous carbons	Meet the needs of psaAWH	Yes	Most are non-toxic	No
CPOs	Meet the needs of psaAWH	Yes	uncertain	Can be large-scale produced

Toxicity<sup>1</sup> refers to the harmful effects on human body or cells. COFs: Covalent organic frameworks; CPOs: crystalline porous organic salts; MOFs: metal-organic frameworks.

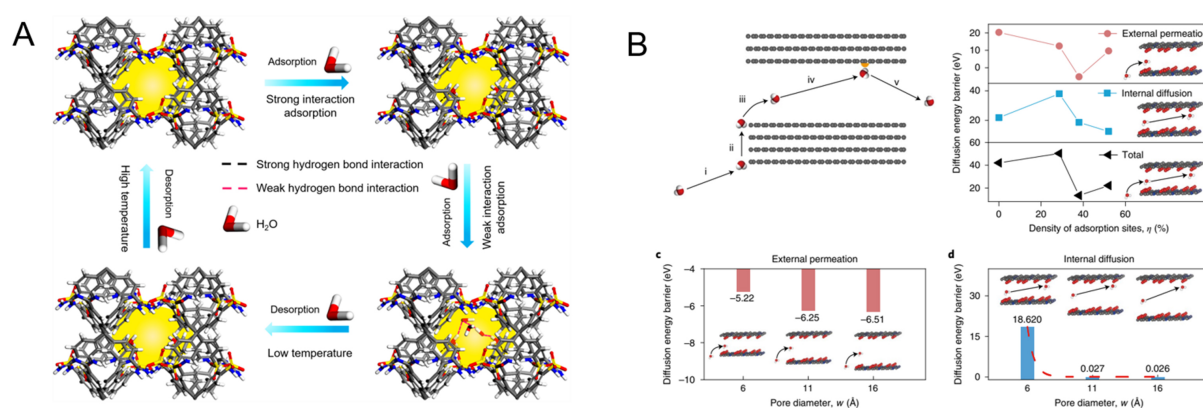


**Figure 27.** (A) Water adsorption/desorption process of CPOS-6. Reproduced with permission<sup>[29]</sup>. Copyright John Wiley and Sons; (B) energy barrier for the diffusion processes of H<sub>2</sub>O in a slit-shaped carbon pore model with various geometric and chemical properties. Reproduced with permission<sup>[151]</sup>. Copyright Springer Nature.

psaAWHs; however, their low water uptake at low RH limits their application. Based on the advantages and disadvantages of different materials, the development of reasonable optimization strategies and the establishment of evaluation criteria for the toxicity, stability, and other commercial indicators will promote the commercialization of psaAWH.

We further evaluated various approaches for regulating the psaAWH performance by modifying the adsorbent structures and properties. By regulating the pore size, functionality, surface area, and crosslinking density, the adsorbent water uptake may be improved, and the shape of the water vapor adsorption isotherm may be adjusted to the applicable RH range. Focus was placed on the kinetic factors of adsorbents, and several strategies for accelerating water adsorption/desorption kinetics were discussed. Many studies have obtained adsorbent materials with rapid kinetic processes by optimizing the adsorption process, intra/inter-crystalline diffusion, and size and shape of the adsorbent. In this section, the intracrystalline diffusion process in microporous adsorbents was examined from a new perspective (superfluidity) for the first time.

Although psaAWH has made considerable progress and demonstrated the potential for alleviating water shortages, there are still some difficulties, and further progress is needed. Extensive efforts have been made to accelerate the adsorption/desorption kinetics of adsorbents, such as the development of hierarchical pore structures, incorporation of photothermal materials, etc. However, these strategies do not fundamentally accelerate the intracrystalline diffusion of water molecules in microporous adsorbents, which is the key to achieving high water absorption at low RH. Based on the previous discussion, the construction of water-molecule superfluid channels in adsorbents is a feasible strategy for solving this problem. It has been reported that the superfluidity of water molecules can be realized by adjusting the size and hydrophilicity of the confined channels<sup>[174]</sup>. In recent reports, it has also been found that the intracrystalline diffusion rate of microporous adsorbents can be improved by adjusting the size of the pore and the number of active sites<sup>[29,151]</sup>. Therefore, based on the mechanism by which superfluidity is generated, reasonable optimization of the adsorbent pores has great potential for realizing water molecule superfluidity in adsorbents and greatly promoting kinetic processes.

## DECLARATIONS

### Authors' contributions

Prepared the manuscript: Zhang S, Ben T

Corrected the manuscript: Fu J, Xing G, Zhu W

### Availability of data and materials

Not applicable.

### Financial support and sponsorship

The research was supported by the National Key R&D Program of China (2021YFA1200400), the National Natural Science Foundation of China (No. 91956108, 21871103, 22001191), the Natural Science Foundation of Zhejiang Province (No. LZ22B010001, LQ23B040003), the Project funded by China Postdoctoral Science Foundation (2022M722829) and the Jinhua Industrial Key Project (2022-3-144).

### Conflicts of interest

Ben T is Junior Editorial Board members of *Chemical Synthesis*. The other authors declare that there are no conflicts of interest.

### Ethical approval and consent to participate

Not applicable.

### Consent for publication

Not applicable.

### Copyright

© The Author(s) 2023.

## REFERENCES

1. Oelkers EH, Hering JG, Zhu C. Water: is there a global crisis? *Elements* 2011;7:157-62. [DOI](#)
2. Ejeian M, Wang RZ. Adsorption-based atmospheric water harvesting. *Joule* 2021;5:1678-703. [DOI](#)
3. Gleick PH. Water in crisis: a guide to the world's freshwater resources. Oxford University Press;1993. pp. 557.
4. Chen K, Tao Y, Shi W. Recent advances in water harvesting: a review of materials, devices and applications. *Sustainability* 2022;14:6244. [DOI](#)
5. Liu X, Beysens D, Bourouina T. Water harvesting from air: current passive approaches and outlook. *ACS Mater Lett* 2022;4:1003-24. [DOI](#)
6. Service RF. Desalination freshens up. *Science* 2006;313:1088-90. [DOI](#) [PubMed](#)

7. Awual MR. Novel ligand functionalized composite material for efficient copper(II) capturing from wastewater sample. *Composites Part B* 2019;172:387-96. [DOI](#)
8. Awual MR. Mesoporous composite material for efficient lead(II) detection and removal from aqueous media. *J. Environ Chem Eng* 2019;7:103124. [DOI](#)
9. Salman MS, Znad H, Hasan N, MM. Optimization of innovative composite sensor for Pb(II) detection and capturing from water samples. *Microchem J* 2021;160:105765. [DOI](#)
10. Shahat A, Kubra KT, Salman MS, Hasan MN, Hasan M. Novel solid-state sensor material for efficient cadmium(II) detection and capturing from wastewater. *Microchem J* 2021;164:105967. [DOI](#)
11. Awual MR. A novel facial composite adsorbent for enhanced copper(II) detection and removal from wastewater. *Chem Eng J* 2015;266:368-75. [DOI](#)
12. Lord J, Thomas A, Treat N, et al. Global potential for harvesting drinking water from air using solar energy. *Nature* 2021;598:611-7. [DOI](#) [PubMed](#)
13. Hanikel N, Prévot MS, Yaghi OM. MOF water harvesters. *Nat Nanotechnol* 2020;15:348-55. [DOI](#) [PubMed](#)
14. Dods MN, Weston SC, Long JR. Prospects for simultaneously capturing carbon dioxide and harvesting water from air. *Adv Mater* 2022;34:2204277. [DOI](#) [PubMed](#)
15. Lu H, Shi W, Guo Y, Guan W, Lei C, Yu G. Materials engineering for atmospheric water harvesting: progress and perspectives. *Adv Mater* 2022;34:2110079. [DOI](#) [PubMed](#)
16. Chen Z, Song S, Ma B, et al. Recent progress on sorption/desorption-based atmospheric water harvesting powered by solar energy. *Energy Mater Sol Cells* 2021;230:111233. [DOI](#)
17. Bagheri F. Performance investigation of atmospheric water harvesting systems. *Water Resour Ind* 2018;20:23-8. [DOI](#)
18. Salehi AA, Ghannadi-Maragheh M, Torab-Mostaedi M, Torkaman R, Asadollahzadeh M. A review on the water-energy nexus for drinking water production from humid air. *Renew Sustain Energy Rev* 2020;120:109627. [DOI](#)
19. Furukawa H, Gándara F, Zhang Y-B, et al. Water adsorption in porous metal-organic frameworks and related materials. *J Am Chem Soc* 2014;136:4369-81. [DOI](#) [PubMed](#)
20. Xu W, Yaghi OM. Metal-organic frameworks for water harvesting from air, anywhere, anytime. *ACS Cent Sci* 2020;6:1348-54. [DOI](#) [PubMed](#)
21. Byun Y, Je SH, Talapaneni SN, Coskun A. Advances in porous organic polymers for efficient water capture. *Chem Eur J* 2019;25:10262-83. [DOI](#) [PubMed](#)
22. Shi W, Guan W, Lei C, Yu G. Sorbents for atmospheric water harvesting: from design principles to applications. *Angew Chem Int Ed* 2022;61:e202211267. [DOI](#) [PubMed](#)
23. Metrane A, Delhali A, Ouikhalfan M, Assen AH, Belmabkhout Y. Water vapor adsorption by porous materials: from chemistry to practical applications. *J Chem Eng Data* 2022;67:1617-53. [DOI](#)
24. Shafeian N, Ranjbar AA, Gorji TB. Progress in atmospheric water generation systems: a review. *Renew Sust Energy Rev* 2022;161:112325. [DOI](#)
25. Li X, Li Z, Xia Q, Xi H. Effects of pore sizes of porous silica gels on desorption activation energy of water vapour. *Appl Therm Eng* 2007;27:869-76. [DOI](#)
26. Fathieh F, Kalmutzki MJ, Kapustin EA, Waller PJ, Yang J, Yaghi OM. Practical water production from desert air. *Sci Adv* 2018;4:eaat3198. [DOI](#) [PubMed](#)
27. Nguyen HL, Hanikel N, Lyle SJ, Zhu C, Proserpio DM, Yaghi OM. A porous covalent organic framework with voided square grid topology for atmospheric water harvesting. *J Am Chem Soc* 2020;142:2218-21. [DOI](#) [PubMed](#)
28. Yilmaz G, Meng FL, Lu W, et al. Autonomous atmospheric water seeping MOF matrix. *Sci Adv* 2020;6:eabc8605. [DOI](#) [PubMed](#)
29. Zhang S, Fu J, Das S, Ye K, Zhu W, Ben T. Crystalline porous organic salt for ultrarapid adsorption/desorption-based atmospheric water harvesting by dual hydrogen bond system. *Angew Chem Int Ed* 2022;61:e202208660. [DOI](#) [PubMed](#)
30. Tang S-Y, Wang Y-S, Yuan Y-F, et al. Hydrophilic carbon monoliths derived from metal-organic frameworks@resorcinol-formaldehyde resin for atmospheric water harvesting. *New Carbon Mater* 2022;37:237-44. [DOI](#)
31. Bulang WG. Solar water recovery from the air. *Solar Energy Int Prog* 1938;3:1526-45. [DOI](#)
32. Aristov TI, Tokarev MM, Gordeeva LG, Snytnikov VN, Parmon VN. New composite sorbents for solar-driven technology of fresh water production from the atmosphere. *Solar Energy* 1999;66:165-8. [DOI](#)
33. Ji JG, Wang RZ, Li LX. New composite adsorbent for solar-driven fresh water production from the atmosphere. *Desalination* 2007;212:176-82. [DOI](#)
34. Kim H, Yang S, Rao R, et al. Water harvesting from air with metal-organic frameworks powered by natural sunlight. *Science* 2017;356:430-4. [DOI](#) [PubMed](#)
35. Kallenberger PA, Fröba M. Water harvesting from air with a hygroscopic salt in a hydrogel-derived matrix. *Commun Chem* 2018;28:1. [DOI](#)
36. Li R, Shi Y, Alsaedi M, Wu W, Shi L, Wang P. Hybrid hydrogel with high water vapor harvesting capacity for deployable solar-driven atmospheric water generator. *Environ Sci Technol* 2018;52:11367-77. [DOI](#) [PubMed](#)
37. Matsumoto K, Sakikawa N, Miyata T. Thermo-responsive gels that absorb moisture and ooze water. *Nat Commun* 2018;9:2315. [DOI](#) [PubMed](#)
38. Lu Z, Wang R, Xia Z, Experimental analysis of an adsorption air conditioning with micro-porous silica gel-water.

- Appl Therm Eng* 2013;50:1015-20. DOI
39. Tashiro Y, Kubo M, Katsumi Y, Meguro T, Komeya K. Assessment of adsorption-desorption characteristics of adsorbents for adsorptive desiccant cooling system. *J Mater Sci* 2004;39:1315-9. DOI
  40. Ng KC, Chua HT, Chung CY, et al. Experimental investigation of the silica gel-water adsorption isotherm characteristics. *Appl Therm Eng* 2001;21:1631-42. DOI
  41. Ng EP, Mintova S. Nanoporous materials with enhanced hydrophilicity and high water sorption capacity. *Micropor Mesopor Mater* 2008;114:1-26. DOI
  42. Resasco DE, Crossley PS, Wang B, White JL. Interaction of water with zeolites: a review. *Catal Rev Sci Eng* 2021;63:302-62. DOI
  43. Wu WD, Zhang H, Men CL. Performance of a modified zeolite 13X-water adsorptive cooling module powered by exhaust waste heat. *Int J Therm Sci* 2011;50:2042-9. DOI
  44. Henninger SK, Ernst SJ, Gordeeva L, et al. New materials for adsorption heat transformation and storage. *Renew Energy* 2017;110:59-68. DOI
  45. Wynnyk KG, Hojjati B, Marriott RA. High-pressure sour gas and water adsorption on zeolite 13X. *Ind Eng Chem Res* 2018;57:15357-65. DOI
  46. Wynnyk KG, Hojjati B, Marriott RA. Sour gas and water adsorption on common high-pressure desiccant materials: zeolite 3A, zeolite 4A, and silica gel. *J Chem Eng Data* 2019;64:3156-63. DOI
  47. Krajnc A, Varlec J, Mazaj M, Ristić A, Logar NZ, Mali G. Superior performance of microporous aluminophosphate with LTA topology in solar-energy storage and heat reallocation. *Adv Energy Mater* 2017;7:1601815. DOI
  48. Klopogge JT, Duong LV, Frost RL. A review of the synthesis and characterisation of pillared clays and related porous materials for cracking of vegetable oils to produce biofuels. *Environ Geol* 2005;47:967. DOI
  49. Zhu HY, Gao WH, Vansant EF. The porosity and water adsorption of alumina pillared montmorillonite. *J Colloid Interf Sci* 1995;171:377. DOI
  50. Aso M, Ito K, Sugino H, et al. Thermal behavior, structure, and dynamics of low-temperature water confined in mesoporous organosilica by differential scanning calorimetry, X-ray diffraction, and quasi-elastic neutron scattering. *Pure Appl Chem* 2013;85:289-305. DOI
  51. Mietner JB, Brieler FJ, Lee YJ, Fröba M. Properties of water confined in periodic mesoporous organosilicas: nanoimprinting the local structure. *Angew Chem Int Ed* 2017;56:12348-51. DOI PubMed
  52. Furukawa H, Cordova KE, O’Keeffe M, Yaghi OM. The chemistry and applications of metal-organic frameworks. *Science* 2013;341:1230444. DOI PubMed
  53. Yaghi OM, Li G, Li H. Selective binding and removal of guests in a microporous metal-organic framework. *Nature* 1995;378:703-6. DOI
  54. Wang Q, Astruc D. State of the art and prospects in metal-organic framework (MOF)-based and MOF-derived nanocatalysis. *Chem Rev* 2020;120:1438-511. DOI PubMed
  55. Qian Q, Asinger QA, Lee MJ, et al. MOF-based membranes for gas separations. *Chem Rev* 2020;120:8161-266. DOI PubMed
  56. Xie S, Monnens W, Wan K, et al. Cathodic electrodeposition of MOF films using hydrogen peroxide. *Angew Chem Int Ed* 2021;60:24950-7. DOI PubMed
  57. Gutiérrez M, Zhang Y, Tan JC. Confinement of luminescent guests in metal-organic frameworks: understanding pathways from synthesis and multimodal characterization to potential applications of LG@MOF systems. *Chem Rev* 2022;122:10438-83. DOI PubMed
  58. Terzopoulou A, Nicholas JD, Chen XZ, Nelson BJ, Pané S, Puigmartí-Luis J. Metal-organic frameworks in motion. *Chem Rev* 2020;120:11175-93. DOI PubMed
  59. He B, Zhang Q, Pan Z. Freestanding metal-organic frameworks and their derivatives: an emerging platform for electrochemical energy storage and conversion. *Chem Rev* 2022;122:10087-125. DOI PubMed
  60. Peng Y, Tan Q, Huang H, et al. Customization of functional MOFs by a modular design strategy for target applications. *Chem Synth* 2022;2:15. DOI
  61. Li H, Li C, Wang Y, et al. Selenium confined in ZIF-8 derived porous carbon@MWCNTs 3D networks: tailoring reaction kinetics for high performance lithium-selenium batteries. *Chem Synth* 2022;2:8. DOI
  62. Nijem N, Canepa P, Kaipa U, et al. Water cluster confinement and methane adsorption in the hydrophobic cavities of a fluorinated metal-organic framework. *J Am Chem Soc* 2013;135:12615-26. DOI PubMed
  63. Nguyen JG, Cohen SM. Moisture-resistant and superhydrophobic metal-organic frameworks obtained via postsynthetic modification. *J Am Chem Soc* 2010;132:4560-1. DOI PubMed
  64. Zhang JP, Zhu AX, Lin RB, Qi XL, Chen XM. Pore surface tailored SOD-type metal-organic zeolites. *Adv Mater* 2011;23:1268-71. DOI PubMed
  65. Yang Q, Vaesen S, Ragon F, et al. A water stable metal-organic framework with optimal features for CO<sub>2</sub> capture. *Angew Chem Int Ed* 2013;52:10316-20. DOI PubMed
  66. Seo YK, Yoon JW, Lee JS, et al. Energy-efficient dehumidification over hierarchically porous metal-organic frameworks as advanced water adsorbents. *Adv Mater* 2012;24:806-10. DOI PubMed
  67. Wade CR, Corrales-Sanchez T, Narayan TC, Dinca M. Postsynthetic tuning of hydrophilicity in pyrazolate MOFs to modulate water adsorption properties. *Energy Environ Sci* 2013;6:2172-7. DOI

68. Wagner JC, Hunter KM, Paesani F, Xiong W. Water capture mechanisms at zeolitic imidazolate framework interfaces. *J Am Chem Soc* 2021;143:21189-94. [DOI](#) [PubMed](#)
69. Choi HJ, Dincă M, Dailly A, Long JR. Hydrogen storage in water-stable metal-organic frameworks incorporating 1,3- and 1,4-benzenedipyrazolate. *Energy Environ Sci* 2010;3:117-23. [DOI](#)
70. Banerjee R, Phan A, Wang B, et al. High-throughput synthesis of zeolitic imidazolate frameworks and application to CO<sub>2</sub> capture. *Science* 2008;319:939-43. [DOI](#) [PubMed](#)
71. Park KS, Ni Z, Côté AP, et al. Exceptional chemical and thermal stability of zeolitic imidazolate frameworks. *Proc Natl Acad Sci USA* 2006;103:10186-91. [DOI](#) [PubMed](#)
72. Tian D, Xu J, Xie ZJ, et al. The first example of hetero-triple-walled metal-organic frameworks with high chemical stability constructed via flexible integration of mixed molecular building blocks. *Adv Sci* 2016;3:1500283. [DOI](#) [PubMed](#)
73. Férey G, Mellot-Draznieks C, Serre C, et al. A chromium terephthalate-based solid with unusually large pore volumes and surface area. *Science* 2005;309:2040-2. [DOI](#) [PubMed](#)
74. Chen Z, Li P, Zhang X, et al. Reticular access to highly porous acs-MOFs with rigid trigonal prismatic linkers for water sorption. *J Am Chem Soc* 2019;141:2900-5. [DOI](#) [PubMed](#)
75. Canivet J, Fateeva A, Guo Y, Coasne B, Farrusseng D. Water adsorption in MOFs: fundamentals and applications. *Chem Soc Rev* 2014;43:5594-617. [DOI](#) [PubMed](#)
76. Liu X, Wang X, Kapteijn F. Water and metal-organic frameworks: from interaction toward utilization. *Chem Rev* 2020;120:8303-77. [DOI](#) [PubMed](#)
77. Dietzel PDC, Johnsen RE, Blom R, Fjellvåg H. Structural changes and coordinatively unsaturated metal atoms on dehydration of honeycomb analogous microporous metal-organic frameworks. *Chem Eur J* 2008;14:2389-97. [DOI](#) [PubMed](#)
78. Ko N, Choi PG, Hong J, et al. Tailoring the water adsorption properties of MIL-101 metal-organic frameworks by partial functionalization. *J Mater Chem A* 2015;3:2057-64. [DOI](#)
79. Hanikel N, Pei X, Chheda S, et al. Evolution of water structures in metal-organic frameworks for improved atmospheric water harvesting. *Science* 2021;374:454-9. [DOI](#) [PubMed](#)
80. Akiyama G, Matsuda R, Sato H, Hori A, Takata M, Kitagawa S. Effect of functional groups in MIL-101 on water sorption behavior. *Micropor Mesopor Mater* 2012;157:89-93. [DOI](#)
81. Deria P, Chung YG, Snurr RQ, Hupp JT, Farha OK. Water stabilization of Zr6-based metal-organic frameworks via solvent-assisted ligand incorporation. *Chem Sci* 2015;6:5172-6. [DOI](#) [PubMed](#)
82. Laha S, Maji TK. Binary/Ternary MOF nanocomposites for multi-environment indoor atmospheric water harvesting. *Adv Funct Mater* 2022;32:2203093. [DOI](#)
83. Xu J, Li T, Chao J, et al. Efficient solar-driven water harvesting from arid air with metal-organic frameworks modified by hygroscopic salt. *Angew Chem Int Ed* 2020;59:5202-10. [DOI](#) [PubMed](#)
84. Hu Y, Fang Z, Wan X, et al. Carbon nanotubes decorated hollow metal-organic frameworks for efficient solar-driven atmospheric water harvesting. *Chem Eng J* 2022;430:133086. [DOI](#)
85. Abtab SMT, Alezi D, Bhatt PM, et al. Reticular chemistry in action: a hydrolytically stable MOF capturing twice its weight in adsorbed water. *Chem* 2018;4:94-105. [DOI](#)
86. Wu Q, Su W, Li Q, Tao Y, Li H. Enabling continuous and improved solar-driven atmospheric water harvesting with Ti<sub>3</sub>C<sub>2</sub>-incorporated metal-organic framework monoliths. *ACS Appl Mater Interf* 2021;13:38906-15. [DOI](#) [PubMed](#)
87. Rieth AJ, Wright AM, Skorupskii G, Mancuso JL, Hendon CH, Dincă M. Record-setting sorbents for reversible water uptake by systematic anion exchanges in metal-organic frameworks. *J Am Chem Soc* 2019;141:13858-66. [DOI](#) [PubMed](#)
88. Karmakar A, Mileo PG, Bok I, et al. Thermo-responsive MOF/polymer composites for temperature-mediated water capture and release. *Angew Chem Int Ed* 2020;59:11003-9. [DOI](#) [PubMed](#)
89. Garzón-Tovar L, Pérez-Carvajal J, Imaz I, Maspoch D. Composite salt in porous metal-organic frameworks for adsorption heat transformation. *Adv Funct Mater* 2017;27:1606424. [DOI](#)
90. Permyakova A, Wang S, Courbon E, et al. Design of salt-metal organic framework composites for seasonal heat storage applications. *J Mater Chem A* 2017;5:12889-98. [DOI](#)
91. Hanikel N, Prévot MS, Fathieh F, et al. Rapid cycling and exceptional yield in a metal-organic framework water harvester. *ACS Cent Sci* 2019;5:1699-706. [DOI](#) [PubMed](#)
92. Wang L, Wang K, An HT, Huang H, Xie LH, Li JR. A hydrolytically stable Cu(II)-based metal-organic framework with easily accessible ligands for water harvesting. *ACS Appl Mater Interf* 2021;13:49509-18. [DOI](#) [PubMed](#)
93. Tao Y, Wu Q, Huang C, et al. Sandwich-structured carbon paper/metal-organic framework monoliths for flexible solar-powered atmospheric water harvesting on demand. *ACS Appl Mater Interf* 2022;14:10966-75. [DOI](#) [PubMed](#)
94. Geng K, He T, Liu R, et al. Covalent organic frameworks: design, synthesis, and functions. *Chem Rev* 2020;120:8814-933. [DOI](#) [PubMed](#)
95. Côté AP, Benin AI, Ockwig NW, O'Keeffe M, Matzger AJ, Yaghi OM. Porous, crystalline, covalent organic frameworks. *Science* 2005;310:1166-70. [DOI](#) [PubMed](#)
96. Freund R, Zaremba O, Arnauts G, et al. The current status of MOF and COF applications. *Angew Chem Int Ed* 2021;60:23975-4001. [DOI](#) [PubMed](#)
97. Das S, Heasman P, Ben T, Qiu S. Porous organic materials: strategic design and structure-function correlation. *Chem Rev*

- 2017;117:1515-63. DOI PubMed
98. Guan X, Chen F, Fang Q, Qiu S. Design and applications of three dimensional covalent organic frameworks. *Chem Soc Rev* 2020;49:1357-84. DOI PubMed
99. Stegbauer L, Hahn MW, Jentys A, et al. Tunable water and CO<sub>2</sub> sorption properties in isostructural azine-based covalent organic frameworks through polarity engineering. *Chem Mater* 2015;27:7874-81. DOI
100. Tan KT, Tao S, Huang N, Jiang D. Water cluster in hydrophobic crystalline porous covalent organic frameworks. *Nat Commun* 2021;12:6747. DOI PubMed
101. Biswal BP, Kandambeth S, Chandra S, et al. Pore surface engineering in porous, chemically stable covalent organic frameworks for water adsorption. *J Mater Chem A* 2015;3:23664-9. DOI
102. Chen Y, Shi Z-L, Wei L, et al. Guest-dependent dynamics in a 3D covalent organic framework. *J Am Chem Soc* 2019;141:3298-303. DOI PubMed
103. Pérez-Carvajal J, Boix G, Imaz I, Maspocho D. The imine-based COF TpPa-1 as an efficient cooling adsorbent that can be regenerated by heat or light. *Adv Energy Mater* 2019;9:1901535. DOI
104. Wang X, Chen L, Chong SY, et al. Sulfone-containing covalent organic frameworks for photocatalytic hydrogen evolution from water. *Nat Chem* 2018;10:1180-9. DOI PubMed
105. Ma J, Fu X-B, Li Y, Xia T, Pan L, Yao Y-F. Solid-state NMR study of adsorbed water molecules in covalent organic framework materials. *Micropor Mesopor Mater* 2020;305:110287. DOI
106. Li W, Xia X, Li S. Screening of covalent-organic frameworks for adsorption heat pumps. *ACS Appl Mater Interf* 2020;12:3265-73. DOI PubMed
107. Gilmanova L, Bon V, Shupletsov L, et al. Chemically stable carbazole-based imine covalent organic frameworks with acidochromic response for humidity control applications. *J Am Chem Soc* 2021;143:18368-73. DOI PubMed
108. Karak S, Kandambeth S, Biswal BP, et al. Constructing ultraporous covalent organic frameworks in seconds via an organic terracotta process. *J Am Chem Soc* 2017;139:1856-62. DOI PubMed
109. Jiang S, Meng L, Ma W, et al. Dual-functional two-dimensional covalent organic frameworks for water sensing and harvesting. *Mater Chem Front* 2021;5:4193-201. DOI
110. Nguyen HL, Gropp C, Hanikel N, Möckel A, Lund A, Yaghi OM. Hydrazine-hydrazide-linked covalent organic frameworks for water harvesting. *ACS Cent Sci* 2022;8:926-32. DOI PubMed
111. Vermonden T, Censi R, Hennink WE. Hydrogels for protein delivery. *Chem Rev* 2012;112:2853-88. DOI PubMed
112. Deng F, Chen Z, Wang C, Xiang C, Poredoš P, Wang R. Hygroscopic porous polymer for sorption-based atmospheric water harvesting. *Adv Sci* 2022;9:2204724. DOI PubMed
113. Guo Y, Bae J, Fang Z, Li P, Zhao F, Yu G. Hydrogels and hydrogel-derived materials for energy and water sustainability. *Chem Rev* 2020;120:7642-707. DOI PubMed
114. Nandakumar DK, Zhang Y, Ravi SK, Guo N, Zhang C, Tan SC. Solar energy triggered clean water harvesting from humid air existing above sea surface enabled by a hydrogel with ultrahigh hygroscopicity. *Adv Mater* 2019;31:1806730. DOI PubMed
115. Yang L, Ravi SK, Nandakumar DK, et al. A hybrid artificial photocatalysis system splits atmospheric water for simultaneous dehumidification and power generation. *Adv Mater* 2019;31:1902963. DOI PubMed
116. Zhao F, Zhou X, Liu Y, Shi Y, Dai Y, Yu G. Super moisture-absorbent gels for all-weather atmospheric water harvesting. *Adv Mater* 2019;31:1806446. DOI PubMed
117. Yang J, Zhang X, Qu H, et al. A moisture-hungry copper complex harvesting air moisture for potable water and autonomous urban agriculture. *Adv Mater* 2020;32:2002936. DOI PubMed
118. Lei C, Guo Y, Guan W, Lu H, Shi W, Yu G. Polyzwitterionic hydrogels for efficient atmospheric water harvesting. *Angew Chem Int Ed* 2022;61:e202200271. DOI PubMed
119. Ni F, Xiao P, Zhang C, Chen T. Hygroscopic polymer gels toward atmospheric moisture exploitations for energy management and freshwater generation. *Matter* 2022;5:2624-58. DOI
120. Hou Y, Sheng Z, Fu C, Kong J, Zhang X. Hygroscopic holey graphene aerogel fibers enable highly efficient moisture capture, heat allocation and microwave absorption. *Nat Commun* 2022;13:1227. DOI PubMed
121. Chang X, Li S, Li N, et al. Marine biomass-derived, hygroscopic and temperature-responsive hydrogel beads for atmospheric water harvesting and solar-powered irrigation. *J Mater Chem A* 2022;10:18170-84. DOI
122. Ni F, Qiu N, Xiao P, et al. Tillandsia-inspired hygroscopic photothermal organogels for efficient atmospheric water harvesting. *Angew Chem Int Ed* 2020;59:19237-46. DOI PubMed
123. Aleid S, Wu M, Li R, et al. Salting-in effect of zwitterionic polymer hydrogel facilitates atmospheric water harvesting. *ACS Mater Lett* 2022;4:511-20. DOI
124. Entezari A, Ejeian M, Wang R. Super atmospheric water harvesting hydrogel with alginate chains modified with binary salts. *ACS Mater Lett* 2020;2:471-7. DOI
125. Xu J, Li T, Yan T, et al. Ultrahigh solar-driven atmospheric water production enabled by scalable rapid-cycling water harvester with vertically aligned nanocomposite sorbent. *Energy Environ Sci* 2021;14:5979-94. DOI
126. Lu K, Liu C, Liu J, et al. Hierarchical natural pollen cell-derived composite sorbents for efficient atmospheric water harvesting. *ACS Appl Mater Interf* 2022;14:33032-40. DOI PubMed
127. Wang M, Sun T, Wan D, et al. Solar-powered nanostructured biopolymer hygroscopic aerogels for atmospheric water harvesting.

- Nano Energy* 2021;80:105569. DOI
128. Li R, Wu M, Shi Y, et al. Hybrid water vapor sorbent design with pollution shielding properties: extracting clean water from polluted bulk water sources. *J Mater Chem A* 2021;9:14731-40. DOI
  129. Yao H, Zhang P, Huang Y, Cheng H, Li C, Qu L. Highly efficient clean water production from contaminated air with a wide humidity range. *Adv Mater* 2020;32:1905875. DOI PubMed
  130. Yu S, Xing GL, Chen LH, Ben T, Su BL. Crystalline porous organic salts: from micropore to hierarchical pores. *Adv Mater* 2020;32:2003270. DOI PubMed
  131. Xing G, Bassanetti I, Bracco S, et al. A double helix of opposite charges to form channels with unique CO<sub>2</sub> selectivity and dynamics. *Chem Sci* 2019;10:730-6. DOI PubMed
  132. Zhao Y, Fan, Pei C, et al. Colossal negative linear compressibility in porous organic salts. *J Am Chem Soc* 2020;142:3593-9. DOI PubMed
  133. Comotti A, Bracco S, Yamamoto A, et al. Engineering switchable rotors in molecular crystals with open porosity. *J Am Chem Soc* 2014;136:618-21. DOI PubMed
  134. Xiao W, Hu C, Ward MD. Guest exchange through single crystal-single crystal transformations in a flexible hydrogen-bonded framework. *J Am Chem Soc* 2014;136:14200-6. DOI PubMed
  135. Liang WB, Carraro F, Solomon MB, et al. Enzyme encapsulation in a porous hydrogen-bonded organic framework. *J Am Chem Soc* 2019;141:14298-305. DOI PubMed
  136. Ami T, Oka K, Tsuchiya K, Tohnai N. Porous organic salts: diversifying void structures and environments. *Angew Chem Int Ed* 2022;61:e202202597. DOI PubMed
  137. Boer SA, Conte L, Tarzia A, et al. Water sorption controls extreme single-crystal-to-single-crystal molecular reorganization in hydrogen bonded organic frameworks. *Chem Eur J* 2022;28:e202201929. DOI PubMed
  138. Xing G, Yan T, Das S, Ben T, Qiu S. Synthesis of crystalline porous organic salts with high proton conductivity. *Angew Chem Int Ed* 2018;57:5345-49. DOI PubMed
  139. Wang H, Shao Y, Mei S, et al. Polymer-derived heteroatom-doped porous carbon materials. *Chem Rev* 2020;120:9363-419. DOI PubMed
  140. Lodewyckx P. The effect of water uptake in ultramicropores on the adsorption of water vapour in activated carbon. *Carbon N Y* 2010;48:2549-53. DOI
  141. Tao Y, Muramatsu H, Endo M, Kaneko K. Evidence of water adsorption in hydrophobic nanospaces of highly pure double-walled carbon nanotubes. *J Am Chem Soc* 2010;132:1214-5. DOI PubMed
  142. Yuan M, Gao M, Shi Q, Dong J. Understanding the characteristics of water adsorption in zeolitic imidazolate framework-derived porous carbon materials. *Chem Eng J* 2020;379:122412. DOI
  143. Zhang E, Hao GP, Casco ME, Bon V, Grätz S, Borchardt L. Nanocasting in ball mills - combining ultra-hydrophilicity and ordered mesoporosity in carbon materials. *J Mater Chem A* 2018;6:859-65. DOI
  144. Liu L, Tan S, Horikawa T, Do DD, Nicholson D, Liu J. Water adsorption on carbon - a review. *Adv Colloid Interf Sci* 2017;250:64-78. DOI
  145. Hao G-P, Mondin G, Zheng Z, et al. Unusual ultra-hydrophilic, porous carbon cuboids for atmospheric-water capture. *Angew Chem Int Ed* 2015;54:1941-5. DOI PubMed
  146. Entezari A, Ejeian M, Wang RZ. Extraordinary air water harvesting performance with three phase sorption. *Mater Today Energy* 2019;13:362-73. DOI
  147. Li R, Shi Y, Wu M, Hong S, Wang P. Improving atmospheric water production yield: enabling multiple water harvesting cycles with nano sorbent. *Nano Energy* 2020;67:104255. DOI
  148. Legrand U, Klassen D, Watson S, et al. Nanoporous sponges as carbon-based sorbents for atmospheric water generation. *Ind Eng Chem Res* 2021;60:12923-12933. DOI
  149. Kumar KV, Preuss K, Guo ZX, Titirici MM. Understanding the hydrophilicity and water adsorption behavior of nanoporous nitrogen-doped carbons. *J Phys Chem C* 2016;120:18167-79. DOI
  150. Byun Y, Coskun A. Epoxy-functionalized porous organic polymers via the diels-alder cycloaddition reaction for atmospheric water capture. *Angew Chem Int Ed* 2018;57:3173-7. DOI PubMed
  151. Song Y, Xu N, Liu G, et al. High-yield solar-driven atmospheric water harvesting of metal-organic-framework-derived nanoporous carbon with fast-diffusion water channels. *Nat Nanotechnol* 2022;17:857-63. DOI PubMed
  152. Guo Y, Guan W, Lei C, Lu H, Shi W, Yu G. Scalable super hygroscopic polymer films for sustainable moisture harvesting in arid environments. *Nat Commun* 2022;13:2761. DOI PubMed
  153. Wright AM, Rieth AJ, Yang S, Wang EN, Dincă M. Precise control of pore hydrophilicity enabled by post-synthetic cation exchange in metal-organic frameworks. *Chem Sci* 2018;9:3856-9. DOI PubMed
  154. Wang H, Yang H, Woon R, Lu Y, Diao Y, D'Arcy JM. Microtubular PEDOT-coated bricks for atmospheric water harvesting. *ACS Appl Mater Interf* 2021;13:34671-8. DOI PubMed
  155. Furukawa H, Ko N, Go YB, et al. Ultrahigh porosity in metal-organic frameworks. *Science* 2010;329:424-8. DOI PubMed
  156. Hu Y, Fang Z, Wan X, et al. Ferrocene dicarboxylic acid ligand-exchanged hollow MIL-101(Cr) nanospheres for solar-driven atmospheric water harvesting. *ACS Sustain Chem Eng* 2022;10:6446-55. DOI
  157. Wang J, Deng C, Zhong G, et al. High-yield and scalable water harvesting of honeycomb hygroscopic polymer driven by natural

- sunlight. *Cell Rep Phys Sci* 2022;3:100954. DOI
158. Zhang Z, Fu H, Li Z, et al. Hydrogel materials for sustainable water resources harvesting & treatment: synthesis, mechanism and applications. *Chem Eng J* 2022;439:135756. DOI
159. Li J, Hu Y, Vlassak J, Suo Z. Experimental determination of equations of state for ideal elastomeric gels. *Soft Matter* 2012;8:8121. DOI
160. Taheri E, Fatehizadeh A, Lima EC, Rezakazemi M. High surface area acid-treated biochar from pomegranate husk for 2,4-dichlorophenol adsorption from aqueous solution. *Chemosphere* 2022;295:133850. DOI
161. Messaoudi NE, Khomri ME, Fernine Y, et al. Hydrothermally engineered *Eriobotrya japonica* leaves/MgO nanocomposites with potential applications in wastewater treatment. *Groundw Sustain Dev* 2022;16:100728. DOI
162. LaPotin A, Kim H, Rao SR, Wang EN. Adsorption-based atmospheric water harvesting: impact of material and component properties on system-level performance. *Acc Chem Res* 2019;52:1588-97. DOI PubMed
163. Dehmani Y, Dridi D, Lamhasni T, Abouarnadasse S, Chtourou R, Lima EC. Review of phenol adsorption on transition metal oxides and other adsorbents. *J Water Process Eng* 2022;49:102965. DOI
164. Bilal M, Sultan M, Morosuk T, et al. Adsorption-based atmospheric water harvesting: a review of adsorbents and systems. *Int Commun Heat Mass Transf* 2022;133:105961. DOI
165. Kim S, Liang Y, Kang S, Choi H. Solar-assisted smart nanofibrous membranes for atmospheric water harvesting. *Chem Eng J* 2021;425:131601. DOI
166. Lyu T, Wang Z, Liu R, Chen K, Liu H, Tian Y. Macroporous hydrogel for high-performance atmospheric water harvesting. *ACS Appl Mater Interf* 2022;14:32433-43. DOI PubMed
167. Chen H, Ran T, Gan Y, et al. Ultrafast water harvesting and transport in hierarchical microchannels. *Nat Mater* 2018;17:935-42. DOI PubMed
168. Wang H-J, Kleinhammes A, McNicholas TP, Liu J, Wu Y. Water adsorption in nanoporous carbon characterized by in situ NMR: measurements of pore size and pore size distribution. *J Phys Chem C* 2014;118:8474-80. DOI
169. Zhang X, Song B, Jiang L. From dynamic superwettability to ionic/molecular superfluidity. *Acc Chem Res* 2022;55:1195-204. DOI PubMed
170. Kapitza P. Viscosity of liquid helium below the  $\lambda$ -point. *Nature* 1938;141:74. DOI
171. Allen JF, Misener A. Flow of liquid helium II. *Nature* 1938;141:75. DOI
172. Gasparini FM, Kimball MO, Mooney KP, Diaz-Avila M. Finite-size scaling of He 4 at the superfluid transition. *Rev Mod Phys* 2008;80:1009. DOI
173. Kolomeisky AB. Channel-facilitated molecular transport across membranes: attraction, repulsion, and asymmetry. *Phys Rev Lett* 2007;98:048105. DOI PubMed
174. Zhang X, Song B, Jiang L. Driving force of molecular/ionic superfluid formation. *CCS Chem* 2021;3:1258-66. DOI
175. Wu K, Chen Z, Li J, Li X, Xu J, Dong X. Wettability effect on nanoconfined water flow. *Proc Natl Acad Sci USA* 2017;114:3358-63. DOI PubMed
176. Yaghi OM, Prevot MS, Hanikel N, Kapustin EA, Fathieh F. Active atmospheric moisture harvester. Available from: <https://patentscope2.wipo.int/search/en/detail.jsf?docId=WO2020036905> [Last accessed on 20 Feb 2023].
177. Yaghi OM, Fathieh F, Kalmutzki MJ, Kapustin EA. Atmospheric moisture harvester. Available from: [https://patentscope2.wipo.int/search/en/detail.jsf?docId=WO2019152962&\\_cid=JP1-LEC9J1-00905-1](https://patentscope2.wipo.int/search/en/detail.jsf?docId=WO2019152962&_cid=JP1-LEC9J1-00905-1) [Last accessed on 20 Feb 2023].
178. Kim H, Yang S, Rao SR, et al. Sorption-based atmospheric water harvesting device. Available from: [https://patentscope2.wipo.int/search/en/detail.jsf?docId=US249457722&\\_cid=JP1-LEC9LR-04379-1](https://patentscope2.wipo.int/search/en/detail.jsf?docId=US249457722&_cid=JP1-LEC9LR-04379-1) [Last accessed on 20 Feb 2023].